On knotted surfaces in R^4

On knotted surfaces in R^4

A dissertation presented

by

Mingyue Chen

to

The Department of Physics

in partial fulfillment of the requirements

for the degree of

Doctor of Philosophy

in the subject of

Physics

Harvard University

Cambridge, Massachusetts

May 2021

Dissertation Advisor:
Professor Cumrun Vafa
Professor Clifford Taubes

Author:
Mingyue Chen

On knotted surfaces in R^4

Abstract

In this article, we study surface knots, and propose some possible generalizations of the crossing changes in classical knot theory to the surface knot theory. In addition, we study the projections of surface knots into R^3 and discuss the double point sets in detail, along with the various moves.

Table of Contents

Title page i
Copyright ii
Abstract iii
List of figures vi
Acknowledgments viii

Introduction **1**

1 Basic Concepts and Visualizations **4**
1.1 Classical knot theory 4
1.1.1 Definition and equivalence 4
1.1.2 Knot diagrams 5
1.1.3 Braids and knots 6
1.2 Surface knots 8
1.2.1 Definition and equivalence 8
1.2.2 The intersection picture 8
1.2.3 The motion picture 10

2 Examples of surface knots and their intersection picture **12**
2.1 Notation 12
2.2 Spun knot 13
2.2.1 Definition 13
2.2.2 Intersection picture (I) 14
2.2.3 Intersection picture (II) 15
2.3 Twist-spun knot 22
2.3.1 Definition 22
2.3.2 Intersection picture 23

3 The Roseman moves and Reidemeister moves **29**
3.1 Intersection curves (*h*-*l* curves) 29
3.2 The Roseman moves 32

4 Crossing changes and generalizations **39**
4.1 A direct approach 39
4.1.1 Preliminaries 39
4.1.2 An example of the chain reaction of crossing changes 43
4.2 The disjoint simple-closed case 47
4.2.1 Arguments in R^4 47
4.2.2 The *h*-*l* curves 49
4.3 The simple closed case 57
4.4 The self-intersecting case 57

References **61**

List of Figures

1.1 The trefoil knot 4
1.2 The Reidemeister moves type I, II, and III 6
1.3 Example of a braid and its closed braid representing the trefoil knot 7
1.4 Two equivalent drawings of a Whitney umbrella 9
1.5 Example of a band sum 11

2.1 Example of a knot 13
2.2 Parametrization of S^2 by the (t, θ) coordinates. The parameter space rolls up vertically and the top and bottom edges (shown in red) map to a meridian. The left and right edges (shown in blue) shrink to the south and north poles respectively. 14
2.3 Example of the intersection curves of a spun knot 15
2.4 Example of the intersection curves of a spun knot 15
2.5 The spinning trajectories of the x_3 and x_4 coordinates of a pair of double points in the knot diagram of k 16
2.6 An example of perturbing k in the spun knot 17
2.7 Four pairs of points associated with one double point in the original knot diagram of k. The z-axis points outward of the page, different from figure 2.6. The arrows represent the direction in the knot k in which t increases. 18
2.8 Illustration of the generation of the four pairs of intersection curves 18
2.9 The intersection curves of the spun trefoil knot 21
2.10 An example of k, p, R_θ and $\tilde{R}_\theta$ 22
2.11 Local intersection curve structures of the twist-spun knot K corresponding to Reidemeister moves of the knot k. The y-axis points outward of the page. . . 24
2.12 A knot diagram as a closed braid 25
2.13 Illustration of the stages of one full twist of k and the intersection curves of K. The y-axis points outward of the page, same as figure 2.11 but different from figure 2.12. 25
2.14 Intersection curves of a twist spun knot, following the stages in figure 2.13. . 28

3.1 Illustration of a triple point as a triplet of intersections among the h-l curves 31

3.2 Roseman moves projected in R^3 [Ros98, Figure 1] 33
3.3 Moves of the *h*-*l* curves due to Roseman moves [Ros98, Figure 2] 34
3.4 Realizations of Reidemeister moves by Roseman moves 36
3.5 Situations where Reidemeister moves are not allowed 38

4.1 A crossing change on a knot diagram of the trefoil knot (figure 1.1) at the double point marked by red, resulting in a knot diagram that represents the trivial knot 39
4.2 An examples of triple points allowing or obstructing a crossing change between h_0 and l_0 41
4.3 Another example of triple points allowing or obstructing a crossing change between h_0 and l_0 42
4.4 A chain reaction of crossing changes 43
4.5 A sequence of Reidemeister moves that turns the trefoil knot over 44
4.6 The *h*-*l* curves of the 1-twist spun trefoil knot 45
4.7 An illustration of the ambient isotopy in the 3-ball $\tilde{B_0}$ 48
4.8 The intersections of h_0 and l_0 with other *h*-*l* curves 49
4.9 An example of the algorithm in theorem 4.2 and the curve generated 51
4.10 Illustration of the correspondence between the number of elements in I and the number of twists in a band neighborhood of $\tau \circ K(c(i_0, i_m))$. 54
4.11 An example of the zero-twist band 54
4.12 An example of a two-twist band as in figure 4.9 56
4.13 A surgery in knot theory that removes part of the knot (the red part) and glues the rest together at a crossing 58
4.14 Illustration of Step 1, in the surgery to a self-intersecting h_0 58
4.15 Illustration of Step 2, in the surgery to a self-intersecting h_0 59
4.16 Illustration of Step 3, in the surgery to a self-intersecting h_0 60

Acknowledgments

I am extremely grateful to my advisor, Professor Clifford Taubes, for guiding me into the field of mathematics, and for his continuous support and patience through all my PhD years. I would also like to thank Professor Cumrun Vafa and Professor John Huth for their warm support.

Introduction

The classical knot theory originated from real-world observations and studies the mathematical object of embedded circles in the three-dimensional Euclidean spaces. Artin initiated the study of embedded surfaces (surface knots) in four-dimensional spaces by proposing the construction of spinning a classical knot in R^3 into a surface in R^4 [Art25].

There are many aspects where surface knots appear as the one-dimensional higher generalization of the classical knots with parallel properties. For example, the knot group is an important algebraic structure in both classical and surface knot theory, which is defined as the fundamental group (π_1) of the complement of a knot (or surface knot) in the ambient space R^3 (or R^4). In both cases, it can be computed schematically via the Wirtinger presentation. Conceptually, this technique views the knotted object by projecting it to the one-dimensional lower version of the ambient space, assigns a group generator to each connected, embedded subset of the projected object, and assigns group relations according to the double point sets. It has long been known that in classical knot theory, an infinite cyclic knot group is the sufficient and necessary condition for a knot to be trivial. See for example [BZH13, proposition 3.10] and [Kaw12, corollary 6.1.5] for proofs. However, the parallel conjecture for surface knots (namely the Unknotting Conjecture) was not proved until recently [Kaw20].

Surface knot theory served as a tool for studying classical knot theory in the particular fields of slice knots and knot cobordism, since both consider surfaces with knot boundaries [FM66]. This originated the description of surface knots using movies [Fox62], i.e., by slicing R^4 into $R^3 \times R$ where the last R is viewed as "time". The surface knot is then

describing as a "movie" of multiple knots (as opposed to a surface) in R^3 where singularities only occur at particular times. Kawauchi further studied this description and proposed the normal form which every surface in R^4 can be made into by isotopy [KS82].

A classical effort in knot theory was to tabulate all possible knots within a certain number of crossings in their knot diagrams (i.e., a diagram of the knot projected on a plane with transverse crossings over and under itself). Conway invented an efficient notation and led to one of the major advances in such efforts [Con70]. Parallel progresses exist in surface knot theory. Yoshikawa invented the marked vertex diagrams, a notation for surface knots based on the foundation of the movies description, that fostered an efficient tabulation of surface knots [Yos94]. Using these diagrams, recent progress has also been made for surface links [Kim20].

On the other hand, broken surface diagrams, a direct generalization of knot diagrams, is another method of representing surface knots. This method projects surface knots to R^3 as immersions (possibly except for at finitely many points), and additionally records the over and under crossings on each connected component of the double point set. One of the merits of this description is that it allows the generalization of the Reidemeister moves in classical knot theory to the Roseman moves of surface knots [Ros98], which describes a collection of moves in the classical or surface knot diagram such that any two diagrams representing an equivalent knot (or surface knot) are related by a collection of these moves. Roseman also generalized these moves to higher dimensions [Ros04].

One of the areas where classical and surface knot theories exhibit opposite properties is in the lifting problems. There are two different lifting problems. In classical knot theory, any immersed closed curve (immersed S^1) in R^2 can be lifted to represent a knot (embedded S^1) in R^3. This is false for immersed S^n's in R^{n+1} for all $n \geq 2$. Ogasa provided the negative proof for $n > 2$ [Oga01]. Proofs for $n = 2$ and some discussions of the conditions when this is allowed are made in [Gil82], [CS98] and [Sat00].

Another lifting problem asks whether a knot diagram can be changed into the trivial knot by a collection of flips of its crossings. This is also true in the classical knot theory.

Since not every immersed $S^n \subset R^{n+1}$ can be lifted to R^{n+2}, the analogous problem in higher dimensions becomes whether the projection of any knotted $S^n \subset R^{n+2}$ down to R^{n+1} can be lifted back to an unknotted n-sphere in R^{n+2}. This is also proved to be false for $n > 2$ by Ogasa [Oga01]. In dimension $n = 2$, the problem is still open [KY15]. There are positive results in some special cases, for example in [Tan04].

This article mainly adopts the broken surface description of surface knots and studies the structures of the double point sets in various examples, and under various moves. In addition, some generalizations to the crossing changes are discussed which are moves and surgeries that changes a surface knot to a related one by using one particular pair of crossings of the knot diagram while preserving the rest of the surface. The article is arranged as follows.

Chapter 1 introduces the basic definitions in classical and surface knot theory. The two sections in this chapter are arranged in a parallel order to emphasize the underlying similarities and differences of the two subjects. The "motion picture" refers to the "movies" in the above introduction and the "intersection picture" refers to the double point set structure obtained from the broken surface description. Chapter 2 explains some important examples of surface knots and studies their double point sets. Chapter 3 discusses Roseman moves for surface knots and their effects on the double point sets. A relation between the Roseman moves and the Reidemeister moves is observed. Chapter 4 studies crossing changes. In particular, the obstructions to an arbitrary crossing change is being discussed and generalizations of crossing changes are proposed. Their effects on the double point sets are also discussed.

Chapter 1

Basic Concepts and Visualizations

In this chapter, the definitions of knots and surface knots are introduced and tools of describing these objects are discussed.

1.1 Classical knot theory

1.1.1 Definition and equivalence

Definition 1.1 (Knot)**.** *A knot is the image of a smooth embedding of S^1 in R^3. A link with n components is a set of n mutually disjoint knots.*

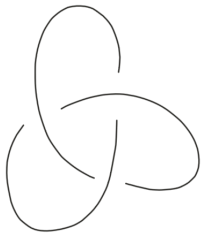

Figure 1.1: *The trefoil knot*

Figure 1.1 is an example of a knot named the trefoil knot. In this section, all the discussions for knots apply equally for links, unless otherwise noted.

Definition 1.2 (Equivalence of knots)**.** *Two knots k and k′ are equivalent if and only if they are*

ambient-isotopic in R^3. An ambient isotopy between k and k′ is a continuous map $F : R^3 \times [0,1] \mapsto R^3$ such that $F(\cdot, 0) = id_{R^3}$, $F(\cdot, s)$ is a homeomorphism of R^3 to itself for all $s \in [0,1]$, and $F(k,1) = k'$. It is clear that ambient isotopy is an equivalence relation. When two knots are equivalent, they are referred to as the same knot.

Conceptually, a knot is considered the same under free deformations of the strand in R^3 without breaking it.

Two links are equivalent only if they have the same number of components.

1.1.2 Knot diagrams

Knots are often represented by knot diagrams.

Definition 1.3 (Knot diagram)**.** *A knot diagram is the image of a knot under the natural projection $(x, y, z) \mapsto (x, y)$ from R^3 to R^2 in general position, together with information on the double points. It is the image of an immersed closed curve in R^2 with finitely many self-intersections at the double points that are all transverse and no multiple points of higher multiplicity. At each double point, the crossing information is being indicated.*

Figure 1.1 is an example of representing a knot by a knot diagram. A knot diagram uniquely represents a knot, but each knot is represented by different knot diagrams. The following theorem describes the situation where two knot diagrams represent the same knot.

Theorem 1.1 (Reidemeister moves)**.** *Two knot diagrams represent the same knot if and only if they are related by a finite sequence of local Reidemeister moves and their inverses, along with isotopies in R^2. The Reidemeister moves are defined in figure 1.2.*

(a) *type I and inverse*

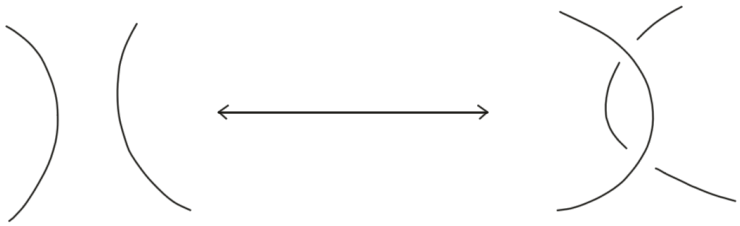

(b) *type II and inverse*

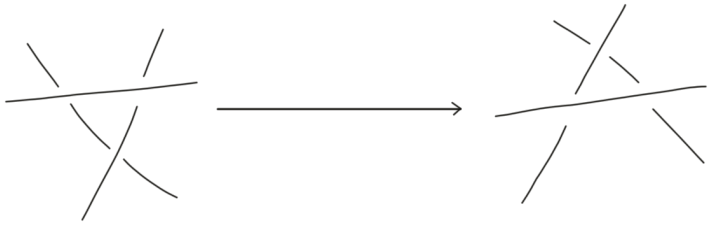

(c) *type III*

Figure 1.2: *The Reidemeister moves type I, II, and III*

The Reidemeister type III move is its own inverse since they only differ by a rotation of the point of view, which is an isotopy in R^2.

Discovery of the Reidemeister moves dates back to 1927 [Rei27]. Kawauchi [Kaw12, Appendix A] and Burde and Zieschang [BZH13, Proposition 1.11, Section 1B] presented rigorous proofs of theorem 1.1 respectively.

1.1.3 Braids and knots

Braids are objects closely related to knots and links.

Definition 1.4 (Braid). *A braid of n strands is the image of n mutually disjoint smooth embeddings f_i of $I = [0,1]$ in $R^2 \times [0,1]$ such that for all $1 \leq i \leq n$,*

- $f_i(0) \in \{(x,0,0) \mid x \in Z,\ 1 \leq x \leq n\}$, $f_i(1) \in \{(x,0,1) \mid x \in Z,\ 1 \leq x \leq n\}$; *and*
- f_i *is strictly increasing in the z-coordinate.*

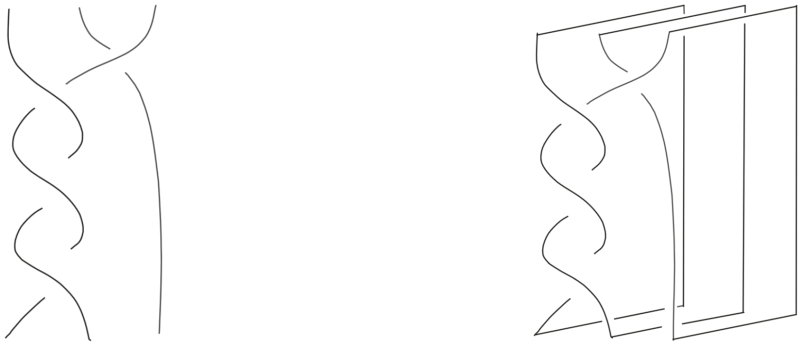

(a) **(b)**

Figure 1.3: *Example of a braid and its closed braid representing the trefoil knot*

Figure 1.3(a) is an example of a braid. Same as knots, equivalence of braids are defined based on ambient isotopy, with additional requirements.

Definition 1.5 (Equivalence of braids)**.** *Two braids are equivalent if and only if they are ambient-isotopic in $R^2 \times [0,1]$ fixing $R^2 \times \{0,1\}$ pointwisely throughout the ambient isotopy.*

Analogous to knots, a braid is considered equivalent under free deformations in R^3 without breaking the strands, with the additional requirements of not moving their endpoints or wrapping any strand over an endpoint. Otherwise, all braids would become trivial.

A theorem by Alexander shows that braids and knots are closely related [Ale23].

Theorem 1.2 (Knots and closed braids)**.** *Every knot is represented by a closed braid* [Ale23]. *A closed braid is a braid with the top and bottom endpoints being connected in pairs in order, far away from (and thus unknotted with) the original braid and in a mutually unknotted way. Specifically, a braid in definition 1.4 is closed up by adding the union of the line segments $\overline{A_i a_i}$, $\overline{a_i b_i}$ and $\overline{b_i B_i}$ for all $1 \leq i \leq n$, where $A_i = \{i,0,0\}$, $a_i = \{i,M,0\}$, $b_i = \{i,M,1\}$ and $B_i = \{i,0,1\}$ and M is chosen larger than the maximum y-coordinate of the original braid, up to smoothing the corners.*

Figure 1.3(b) is the closed braid of figure 1.3(a). It represents the trefoil knot shown in figure 1.1.

Similar to knot diagrams, a closed braid uniquely represents a knot, but each knot is represented by different closed braids, even with different numbers of strands.

Although braids in figure 1.3 are represented in a similar way as knot diagrams, braids are also completely algebraically defined by all the crossing information between the strands. Therefore, closed braids serve as a representation of knots independently from knot diagrams.

Adams [Ada94, Section 5.4] provides a comprehensive analysis of braids and a proof of theorem 1.2.

1.2 Surface knots

Surface knots are knotted objects in R^4. We restrict to the oriented case. In this section, subjects are arranged in parallel with section 1.1 for comparison.

1.2.1 Definition and equivalence

Definition 1.6 (Surface knot)**.** *A surface knot is the image of a smooth embedding of an oriented connected closed surface in R^4.*

Definition 1.7 (Equivalence of surface knots)**.** *Two surface knots K and K' are equivalent and referred to as the same if and only if they are ambient-isotopic in R^4.*

When two surface knots are equivalent, their underlying types of surfaces are the same.

1.2.2 The intersection picture

In the intersection picture, a surface knot is projected from R^4 to R^3 by $\tau(x_1, x_2, x_3, x_4) = (x_1, x_2, x_3)$. Giller proved that the projection is always an immersion, possibly after ambient isotopy of the original surface knot [Gil82]. In contrary to the case of knot diagrams, this is a less obvious result.

Theorem 1.3 (Intersection picture)**.** *Any oriented surface knot can be ambient-isotoped such that its projection under τ is the image of an immersion in R^3* [Gil82]*. The multiple point set consists of finitely many pairs of closed curves. There are two types of points on these curves.*

- *The intersections among these curves (including self-intersections) are all transverse and are exactly the triple points of the immersion.*
- *The other points on the curves are exactly the double points of the immersion.*

Without allowing ambient isotopy, the projection of any surface knot in general position to R^3 is the image of an immersion except possibly at finitely many points, named the branch points [Whi44]. It is often useful to discuss branch points even though they are not essential (i.e., they can be removed according to theorem 1.3).

Definition 1.8 (Whitney umbrella)**.** *A Whitney umbrella is the neighborhood of a pinch point singularity of a smooth surface in R^3. Specifically, the surface can be put into the parametric form $(u, v) \mapsto (u, v^2, uv)$ in this neighborhood.*

Figure 1.4: *Two equivalent drawings of a Whitney umbrella*

Figure 1.4 (a) and (b) are both Whitney umbrellas, equivalent up to smoothing the corner in (b).

A similar description follows for the intersection picture (comparing with theorem 1.3).

Theorem 1.4 (Intersection picture with branch points)**.** *Any surface knot in general position projects under τ to the image of an immersion in R^3 except possibly at finitely many points. The multiple point set consists of finitely many pairs of curves. Each pair of the curves are either both*

closed or share both endpoints, named the branch points. There are three types of points on these curves.

- *The branch points are exactly where the mapping fails to be an immersion.*
- *The intersections among these curves (including self-intersections) other than the branch points are all transverse and are exactly the triple points of the immersion.*
- *The rest of points on the curves are exactly the double points of the immersion.*

These curves are named the intersection curves since they describe the multiple point set of the immersion. They are the main object of this article.

Parallel to the Reidemeister moves, there is a collection of moves, the Roseman moves [Ros98], that completely describes the equivalence between surface knots in the intersection picture. They are discussed in Chapter 3.

1.2.3 The motion picture

Motion picture describes a surface knot K by slicing $R^4 = R^3 \times R$ and presenting the intersections $K \cap (R^3 \times \{x_4\})$ at all x_4-levels. Based on Morse theory, for a surface knot in general position, the topology of such intersections (regarded as images of embeddings in R^3) changes finitely many times while x_4 screens through R. This compares with the closed braid representation of knots. Starting from the bottom, the strands intertwine finitely many times as the z-coordinate increases monotonically.

Definition 1.9 (Band sum)**.** *Let l be an oriented link in R^3. Let B be an oriented D^2 embedded in R^3 with two connected, disjoint arcs α and β on ∂B such that $B \cap l = \partial B \cap l = \alpha \cup \beta$ and that the orientations of α and β inherited from B match the orientation of l. Then B is called a band on the link l. The new oriented link $l' = \overline{(l \cup \partial B) - (\alpha \cup \beta)}$, with the natural orientation matching that of l and ∂B, is called the link obtained from l by the band sum along B. It is denoted as $l' = s(l; B)$. (See figure 1.5.)*

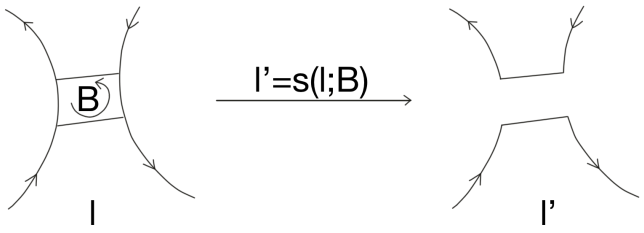

Figure 1.5: *Example of a band sum*

Theorem 1.5 (Motion picture)**.** *For any surface knot K in R^4, there exists:*

- *Two collections, D and D', of respectively n and n' mutually disjoint D^2 embedded in R^3; and*
- *A collection $B = \{B_1, \cdots, B_m\}$ of mutually disjoint bands on the trivial link $l_0 = \partial D$ such that for all $1 \leq i \leq m$, $l_i = s(l_{i-1}; B_i)$ and $l_m = \partial D'$,*

such that K is ambient-isotopic, up to smoothing the corners, to the union of:

$$(D \times \{0\}) \cup \bigcup_{i=1}^{m} \left(B_i \times \{\frac{i}{m+1}\} \right) \cup \bigcup_{i=0}^{m} \left(l_i \times \left[\frac{i}{m+1}, \frac{i+1}{m+1} \right] \right) \cup (D' \times \{1\}).$$

Conceptually, a surface knot is represented by a finite collection of band sums occurring at different x_4-levels, closed up with top and bottom caps. The collection of D, D' and B uniquely represents a surface knot, but each surface knot has different motion picture representations.

Both the closed braid representation of knots and the motion picture representation of surface knots have a close relation with Morse theory [Mil16]. Furthermore, Kawauchi [KS82] proved a normal from of the motion picture description of surface knots.

Chapter 2

Examples of surface knots and their intersection picture

In this chapter, several examples of surface knots are constructed and the structure of their intersection curves are described.

2.1 Notation

Let $I = [0,1]$ and $R^3_+ = \{(x,y,z) \in R^3 \mid z \geq 0\}$.

In this chapter, coordinates in R^3 and R^4 are denoted by (x,y,z) and (x_1,x_2,x_3,x_4) respectively. Each coordinate is also used notationally as a function from the space to R.

Definition 2.1. *Let X and Y be two manifolds with boundary. An embedding of $(X,\partial X)$ in $(Y,\partial Y)$ is an embedding of X in Y mapping ∂X to ∂Y and $int(X)$ to $int(Y)$.*

Lemma 2.1. *Parametrize S^1 by $[0,2\pi]/\{0,2\pi\}$ in the natural way. Any smooth embedding k of S^1 in R^3 is ambient-isotopic to the following form, up to smoothing the corners:*

- *$k|_{[0,1]}$ is a smooth embedding of $(I,\partial I)$ in $(R^3_+,\partial R^3_+)$; and*
- *$k|_{[1,2\pi]}$ is a linear function from $[1,2\pi]$ to the $z=0$ plane.*

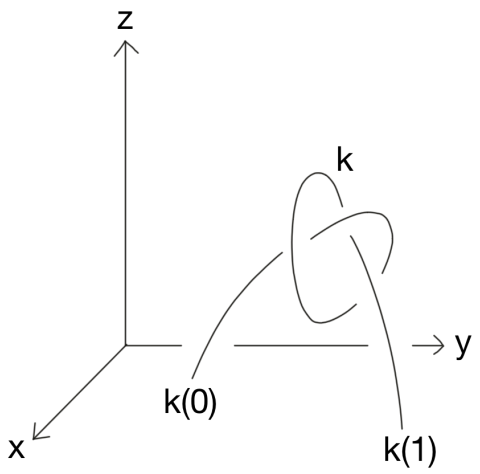

Figure 2.1: *Example of a knot*

In this chapter, a knot k is regarded as a smooth embedding (as opposed to its image) of $(I, \partial I)$ (as opposed to S^1) in $(R^3_+, \partial R^3_+)$. See figure 2.1. Equivalently, $z(k(0)) = z(k(1)) = 0$ and $z(k(t)) > 0$ for all $t \in (0,1)$. By lemma 2.1, this embedding does not lose any information about the original knot.

2.2 Spun knot

Construction of the spun knots was introduced by Artin [Art25].

2.2.1 Definition

Definition 2.2. *The spinning function* $Spin : R^3 \times [-\pi, \pi] \mapsto R^4$ *maps* $(x, y, z; \theta)$ *to* $(x, y, z\cos\theta, z\sin\theta)$.

Definition 2.3 (Spun knot)**.** *Given a knot* $k : (I, \partial I) \mapsto (R^3_+, \partial R^3_+)$*, the spun knot* K *of* k *is an embedding of* S^2 *in* R^4*:*

$$K(t, \theta) = Spin\big(k(t); \theta\big),$$

where S^2 *is parametrized by the map* $(t, \theta) \mapsto (s\cos\theta, s\sin\theta, t)$ *from* $I \times [-\pi, \pi]$ *to* $S^2 \subset R^3$ *where* $s = \frac{1}{2}\sqrt{4t(1-t)}$*. (See figure 2.2.)*

- *This map is injective because* k *is injective and* $z(k(t)) > 0$ *for* $t \in (0,1)$.

- *This is consistent with the S^2 parametrization because $z(k(0)) = z(k(1)) = 0$.*

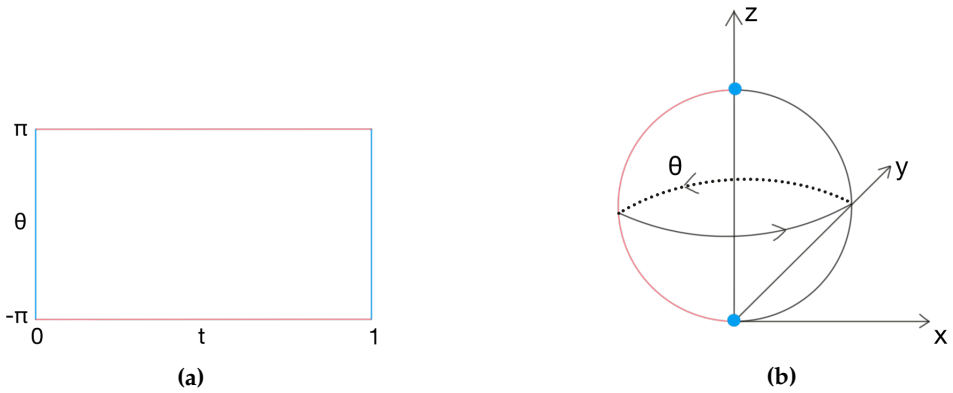

Figure 2.2: *Parametrization of S^2 by the (t, θ) coordinates. The parameter space rolls up vertically and the top and bottom edges (shown in red) map to a meridian. The left and right edges (shown in blue) shrink to the south and north poles respectively.*

From the symmetry of the definition formula of the spun knot, there are two non-equivalent ways of projecting the spun knot $K \subset R^4$ to R^3: along x_1 or x_2, and along x_3 or x_4.

2.2.2 Intersection picture (I)

In this subsection let $\tau(x_1, x_2, x_3, x_4) = (x_1, x_3, x_4)$.

Two points $\overline{A} = K(t_A, \theta_A)$ and $\overline{B} = K(t_B, \theta_B)$ have the same image under τ if and only if

$$\begin{cases} x(k(t_A)) = x(k(t_B)) \\ z(k(t_A)) = z(k(t_B)) \\ \theta_A = \theta_B \end{cases}.$$

Without loss of generality, let the projection $(x, y, z) \mapsto (x, z)$ generate a knot diagram of k. See figure 2.3. Two points (t_A, θ_A) and (t_B, θ_B) in S^2 are double points of K under τ if and only if $\theta_A = \theta_B$ and that $A = k(t_A)$ and $B = k(t_B)$ are a pair of double points in the aforementioned knot diagram of k.

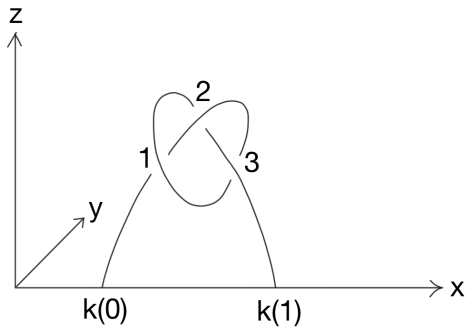

Figure 2.3: *Example of the intersection curves of a spun knot*

The intersection curves are pairs of parallel circles in S^2 of constant t-values. Figure 2.4 shows the intersection curves of the spun knot K of the knot k in figure 2.3. In this notation, each h curve lies exactly above (in terms of the x_2-coordinate) the l curve with the same number, therefore projecting to the same image in R^3 under τ. The subscripts 1 through 3 in figure 2.4 match the numbers of the double points in figure 2.3. For example, as t increases from 0, the first double point in figure 2.3 is the higher (in terms of the y-coordinate) point numbered 1. Therefore, the first curve in figure 2.4 is h_1, starting from the left of the (t, θ) space.

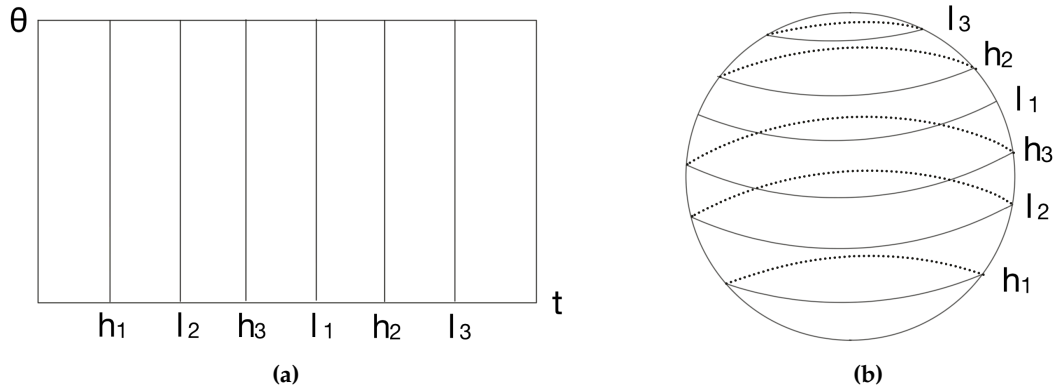

Figure 2.4: *Example of the intersection curves of a spun knot*

2.2.3 Intersection picture (II)

In this subsection let $\tau(x_1, x_2, x_3, x_4) = (x_1, x_2, x_4)$.

Without loss of generality, let the projection $(x, y, z) \mapsto (x, y)$ generate a knot diagram of k.

The two points $\overline{A} = K(t_A, \theta_A)$ and $\overline{B} = K(t_B, \theta_B)$ having the same image under τ requires

$$\begin{cases} x(k(t_A)) = x(k(t_B)) \\ y(k(t_A)) = y(k(t_B)) \end{cases}.$$

Equivalently, a necessary condition is that $A = k(t_A)$ and $B = k(t_B)$ are a pair of double points in the aforementioned knot diagram of k.

Let $z_A = z(A) > z_B = z(B)$ without loss of generality. They create the trajectory in x_3 and x_4 coordinates as shown in figure 2.5.

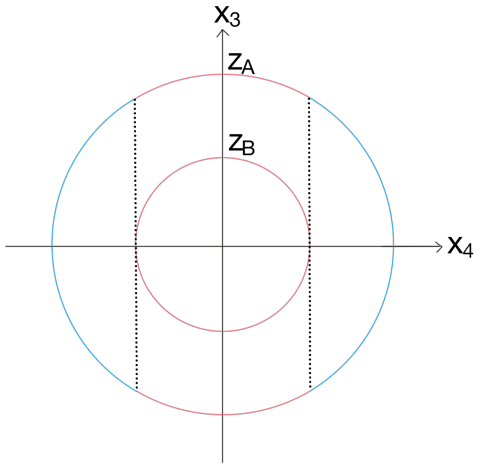

Figure 2.5: *The spinning trajectories of the x_3 and x_4 coordinates of a pair of double points in the knot diagram of k*

This shows that under the projection τ, curves of quadruple points (shown in red in figure 2.5) exist as well as double points (shown in blue in figure 2.5). By theorem 1.4, K is not in general position. The quadruple points are unstable singularities and are removable by an arbitrarily small perturbation of K.

Let an embedding k' of $(I, \partial I)$ in $(R^3_+, \partial R^3_+)$ be slightly pushed off from k. Specifically,

- $k'|_{\partial I} = k|_{\partial I}$;
- $z \circ k' = z \circ k$; and

- k' and k are close enough such that the linear isotopy $F(\cdot, s) = (1-s)k + sk'$ is injective in $int(I) \times [0,1]$.

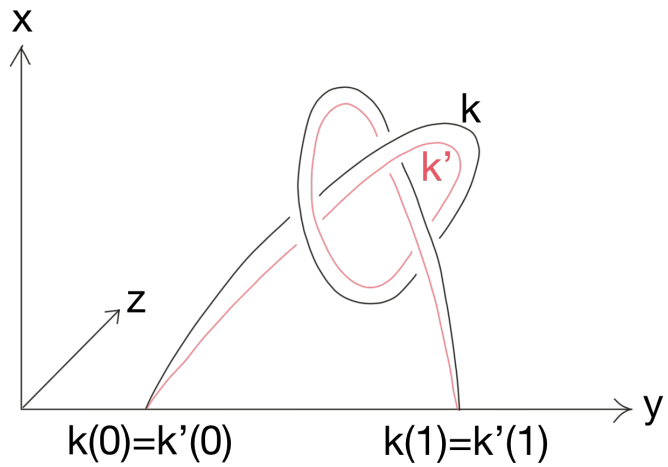

Figure 2.6: *An example of perturbing k in the spun knot*

See figure 2.6. The definition of the spun knot K is perturbed accordingly, up to smoothing the corners ($\theta \in [-\pi, \pi]$):

$$K(t,\theta) = Spin\big(F(t, |\theta/\pi|); \theta\big).$$

Conceptually, the knot deviates in R^3 from k to k' and back, as it goes through a full cycle of spinning into R^4.

Each quadruple of the multiple points in the unperturbed K become four pairs of double points in the perturbed K. Each double point of the original knot diagram of k generates two pairs of intersection curves of K. Consider the spun images of each pair of points in figure 2.7 marked by α, β, γ and δ respectively.

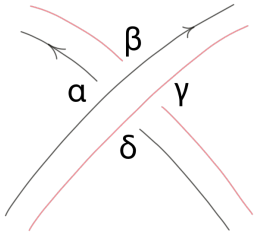

Figure 2.7: *Four pairs of points associated with one double point in the original knot diagram of k. The z-axis points outward of the page, different from figure 2.6. The arrows represent the direction in the knot k in which t increases.*

For each pair of points α through δ, let the upper point (in terms of the z-coordinate) be A and the lower point be B. Let $A = F(t_A, |\theta_A/\pi|)$, $B = F(t_B, |\theta_B/\pi|)$ and $z_A = z(A) > z_B = z(B)$. Specifically, $\theta_A = 0$ or π if A lies on the knot k or k' respectively. Same for B. Their spun images in K are $\overline{A} = K(t_A, \theta_A)$ and $\overline{B} = K(t_B, \theta_B)$.

Figure 2.8 illustrates the structures in detail. In the discussions below, let the z-axis in figure 2.7 point outward of the page.

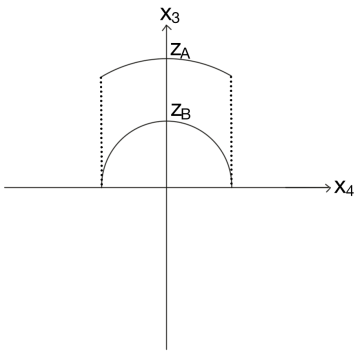

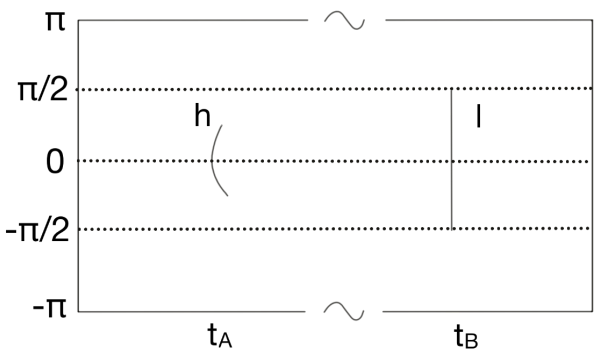

(a) α

Figure 2.8 (Continued on next page): *Illustration of the generation of the four pairs of intersection curves*

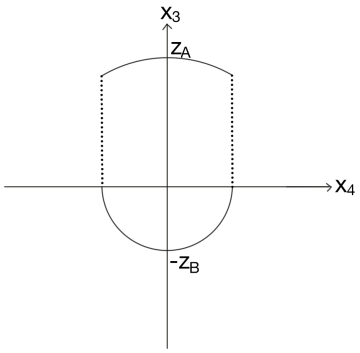

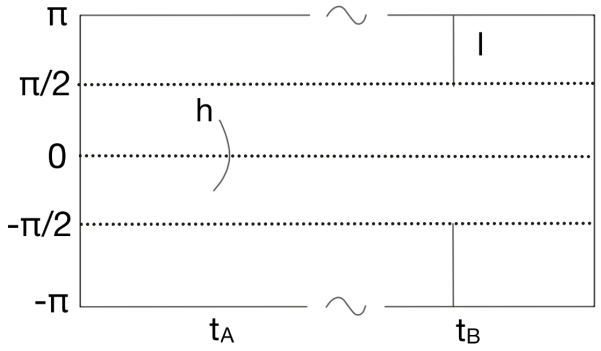

(b) β

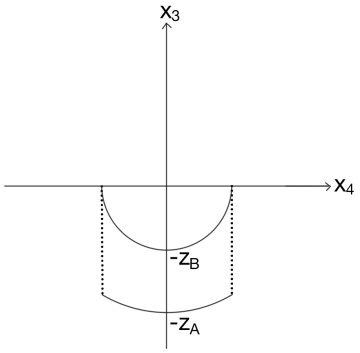

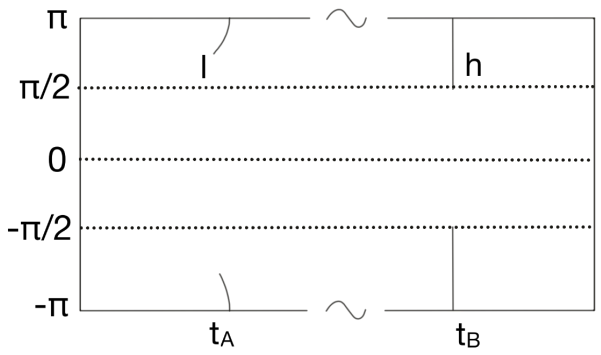

(c) γ

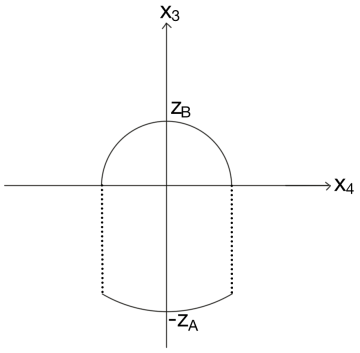

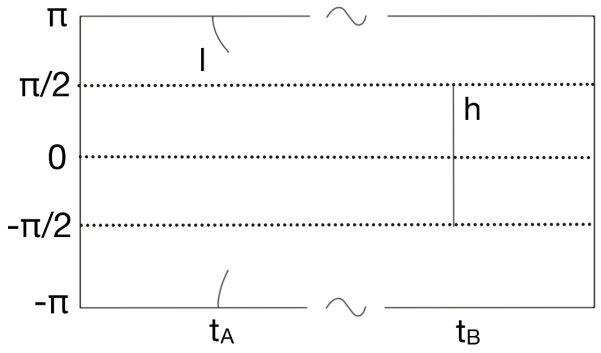

(d) δ

Figure 2.8 (Continued)

- α contains the pair of points $A = k(t_A) = F(t_A, 0)$ and $B = k(t_B) = F(t_B, 0)$. They have the spun images $\overline{A} = K(t_A, 0)$ and $\overline{B} = K(t_B, 0)$. $x_3(\overline{A}) > x_3(\overline{B}) > 0$. They generate a pair of intersection curves as θ_B travels through $[-\frac{\pi}{2}, \frac{\pi}{2}]$ and θ_A dependently through

$[-\arcsin(\frac{z_B}{z_A}), \arcsin(\frac{z_B}{z_A})]$. Notice when θ_B becomes non-zero, both positively and negatively, B deviates from k to k'. In figure 2.7, this corresponds to the horizontal movement of the lower black curve at α towards the lower red curve. The upper point A needs to follow this movement by deviating slightly in the direction along the arrow of the upper black curve. Equivalently, t_A deviates slightly in the increasing direction when θ_B (and therefore θ_A) is non-zero. This is shown in figure 2.8(a). Rigorously, t_B should also deviate slightly, in the decreasing direction of t_B according to figure 2.7, when θ_A is non-zero. However, such movements are ignored in figure 2.8 since they do not affect the essential properties of the curves.

- β contains the pair of points $A = k(t_A) = F(t_A, 0)$ and $B = k'(t_B) = F(t_B, 1)$. They have the spun images $\overline{A} = K(t_A, 0)$ and $\overline{B} = K(t_B, \pi)$. $x_3(\overline{A}) > 0 > x_3(\overline{B})$. They generate a pair of intersection curves as θ_B travels through $[-\pi, -\frac{\pi}{2}] \cup [\frac{\pi}{2}, \pi]$ and θ_A dependently through $[-\arcsin(\frac{z_B}{z_A}), \arcsin(\frac{z_B}{z_A})]$. When θ_B is not equal to $\pm\pi$ on both sides, B deviates from k' to k. In figure 2.7, this corresponds to the horizontal movement of the lower red curve at β towards the lower black curve. The upper point A needs to follow this movement by deviating slightly in the direction against the arrow of the upper black curve. Equivalently, t_A deviates slightly in the decreasing direction when θ_B is not equal to $\pm\pi$ (and therefore θ_A is non-zero). This is shown in figure 2.8(b). They connect with the curves generated by α and form a pair of closed curves. Notice that the deviations of t_A are brought by the perturbation and are essential in the connection of the curves generated by α and β. Without the perturbation, the h curves in figure 2.8 (a) and (b) would coincide, indicating quadruple points.

- γ contains the pair of points $A = k'(t_A) = F(t_A, 1)$ and $B = k'(t_B) = F(t_B, 1)$. They have the spun images $\overline{A} = K(t_A, \pi)$ and $\overline{B} = K(t_B, \pi)$. $0 > x_3(\overline{B}) > x_3(\overline{A})$. They generate a pair of intersection curves as θ_B travels through $[-\pi, -\frac{\pi}{2}] \cup [\frac{\pi}{2}, \pi]$ and θ_A dependently through $[-\pi, -\pi + \arcsin(\frac{z_B}{z_A})] \cup [\pi - \arcsin(\frac{z_B}{z_A}), \pi]$.

- δ contains the pair of points $A = k'(t_A) = F(t_A, 1)$ and $B = k(t_B) = F(t_B, 0)$. They have the spun images $\overline{A} = K(t_A, \pi)$ and $\overline{B} = K(t_B, 0)$. $x_3(\overline{B}) > 0 > x_3(\overline{A})$. They generate

a pair of intersection curves as θ_B travels through $[-\frac{\pi}{2}, \frac{\pi}{2}]$ and θ_A dependently through $[-\pi, -\pi + \arcsin(\frac{z_B}{z_A})] \cup [\pi - \arcsin(\frac{z_B}{z_A}), \pi]$. They connect with the curves generated by γ and form another pair of closed curves.

In conclusion, each double point of the original knot diagram of k generates two pairs of intersection curves of the perturbed K under τ.

Figure 2.9 provides a complete example using the trefoil knot.

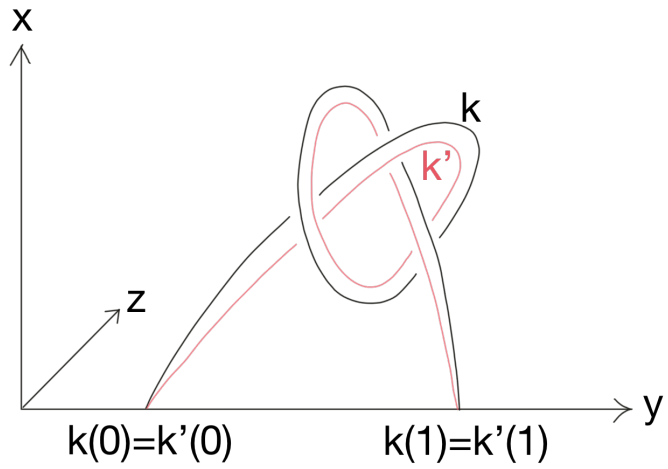

(a) *A knot with perturbation assigned*

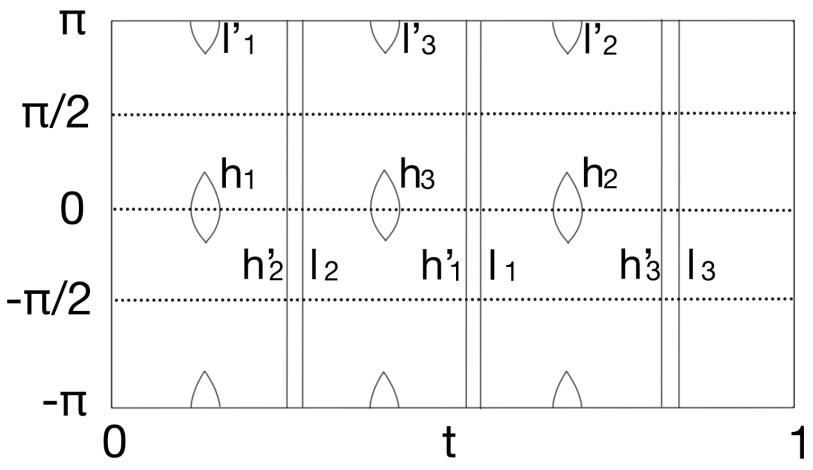

(b) *The intersection curves of the spun knot*

Figure 2.9: *The intersection curves of the spun trefoil knot*

2.3 Twist-spun knot

The construction of the twist-spun knots was introduced by Zeeman [Zee65] in topological language. The definition presented below uses parametrization and rotations in R^3 and is equivalent to the original.

2.3.1 Definition

Let N (S) be the north (south) pole of the unit ball $D^3 \subset R^3$ centered at the origin. For a knot $k : (I, \partial I) \mapsto (R^3_+, \partial R^3_+)$, define an embedding $p : D^3 \mapsto R^3_+$ such that

- $p(N) = k(0)$, $p(S) = k(1)$; and
- $k(int(I)) \subset p(D^3 - \{N, S\}) \subset int(R^3_+)$.

Let $R_\theta(x, y, z) = (x\cos\theta + y\sin\theta, y\cos\theta - x\sin\theta, z)$ be the rotation operator on D^3 along the z-axis.

p pushes forward R_θ to a self-homeomorphism $\tilde{R}_\theta = pR_\theta p^{-1}$ of $p(D^3)$ fixing $p(N)$ and $p(S)$. See figure 2.10.

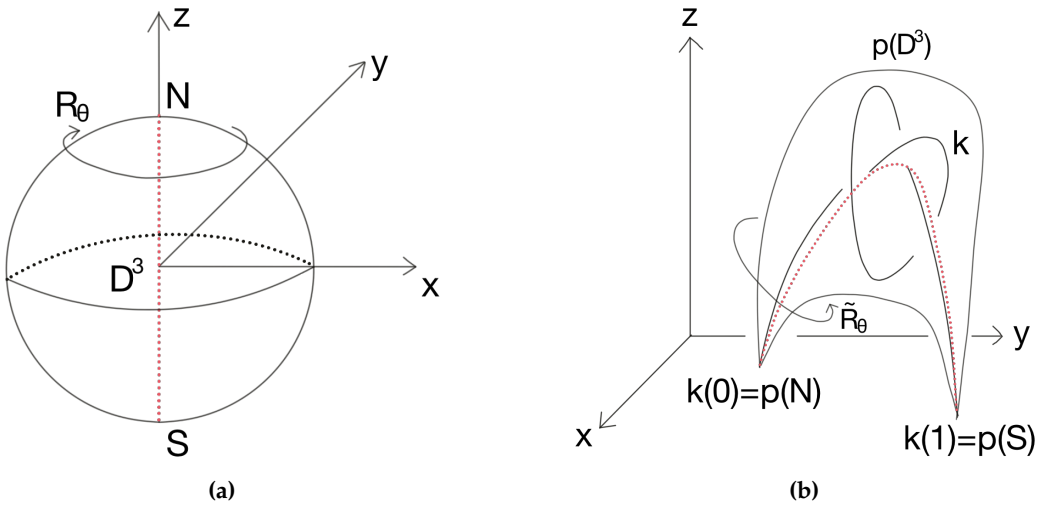

Figure 2.10: *An example of k, p, R_θ and $\tilde{R}_\theta$*

Definition 2.4 (Twist-spun knot)**.** *Given a knot $k : (I, \partial I) \mapsto (R^3_+, \partial R^3_+)$, the m-twist-spun knot*

K of k is an embedding of S^2 in R^4:

$$K(t,\theta) = Spin\big(\tilde{R}_{m\theta}(k(t));\theta\big).$$

- *This map is an injection because $z(\tilde{R}_{m\theta}(k(t))) > 0$ for $t \in (0,1)$ and $\tilde{R}_{m\theta} \circ k$ is always an injection.*
- *This is consistent with the S^2 parametrization because $p(N) = k(0)$ and $p(S) = k(1)$ are fixed under $\tilde{R}_{m\theta}$ and that their z-coordinates are zero.*
- *The spun knot K is independent from the choice of p up to ambient isotopy.*

Conceptually, the knot k is spun to the x_4-coordinate and rotated in R^3 simultaneously. A further theorem by Zeeman shows that the ± 1-twist-spun knots of any knot k is a trivial surface knot that bounds a 3-ball in R^4 [Zee65].

2.3.2 Intersection picture

The intersection picture of twist-spun knots was also studied by Satoh [Sat02]. Here an independent point of view is presented.

For simplicity, let $\tau(x_1, x_2, x_3, x_4) = (x_1, x_3, x_4)$. Let the knot diagram of k be obtained by the projection $(x, y, z) \mapsto (x, z)$.

Since rotations in R^3 preserve the knot, the aforementioned knot diagram undergoes a finite sequence of Reidemeister moves (theorem 1.1). Therefore, the intersection curves of K under τ are the same as the spun knot case in subsection 2.2.2 except at finitely many locations, corresponding to the Reidemeister moves. They start as disjoint straight lines corresponding to the double points of the knot diagram.

Theorem 2.2 (Intersection curves of twist-spun knots (local))**.** *The intersection curves of the twist-spun knot K under τ are disjoint straight lines expect at finitely many points when the knot diagram of k undergoes Reidemeister moves. Each move corresponds to a local structure in figure 2.11.*

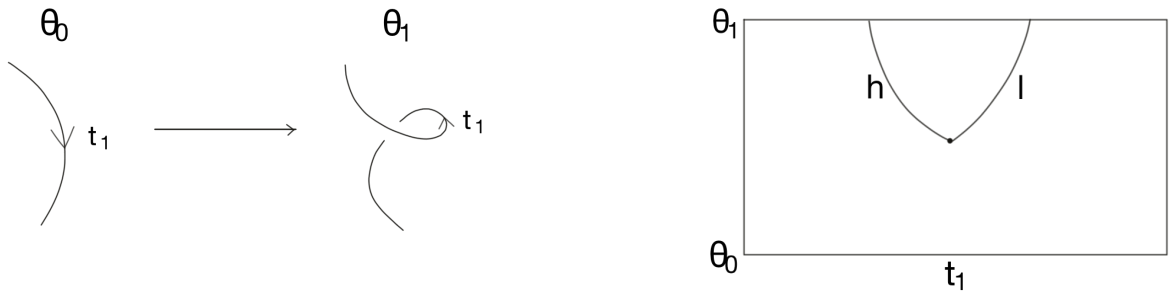

(a) *Reidemeister move I*

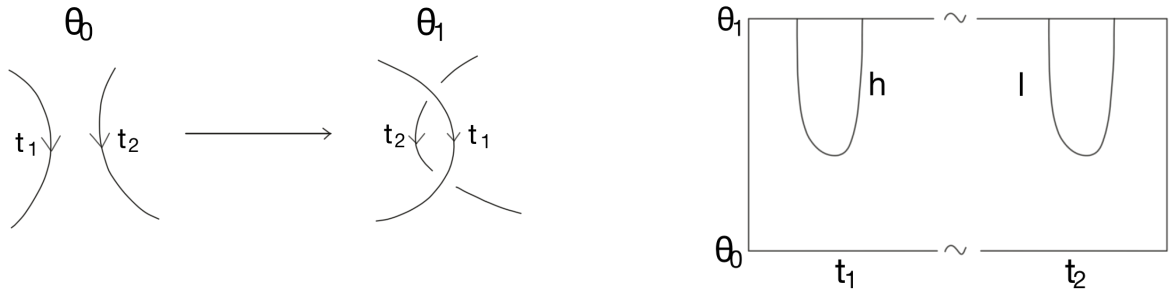

(b) *Reidemeister move II*

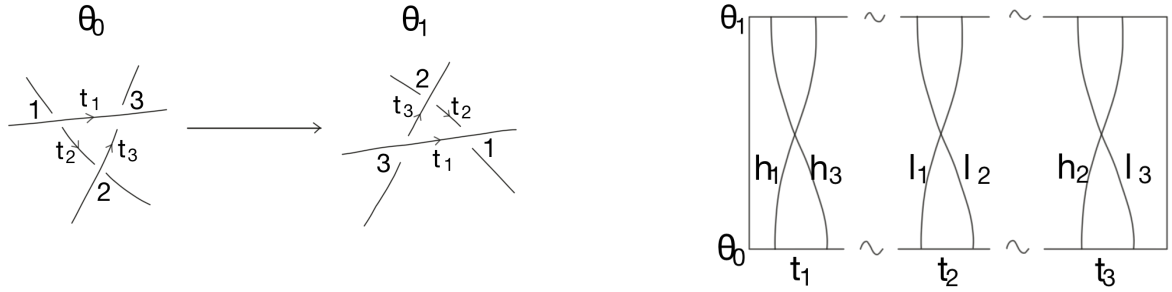

(c) *Reidemeister move III*

Figure 2.11: *Local intersection curve structures of the twist-spun knot K corresponding to Reidemeister moves of the knot k. The y-axis points outward of the page.*

The proof is straightforward since the intersection curves track the double points of the knot diagram at all times and through the Reidemeister moves as well.

Globally, a knot has a closed braid configuration (theorem 1.2). Slightly shift the closing strands in theorem 1.2 in the x-direction before projecting the closed braid by $(x, y, z) \mapsto (x, z)$. Without loss of generality, consider a knot k in figure 2.12.

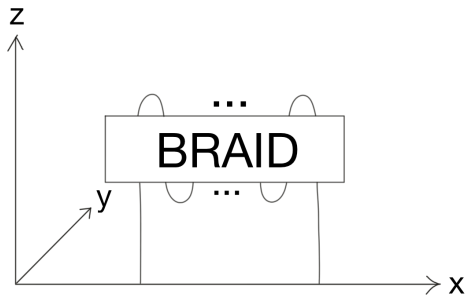

Figure 2.12: *A knot diagram as a closed braid*

Figure 2.13 illustrates the stages k goes through to perform a rotation in R^3 and the structures of the intersection curves of K generated.

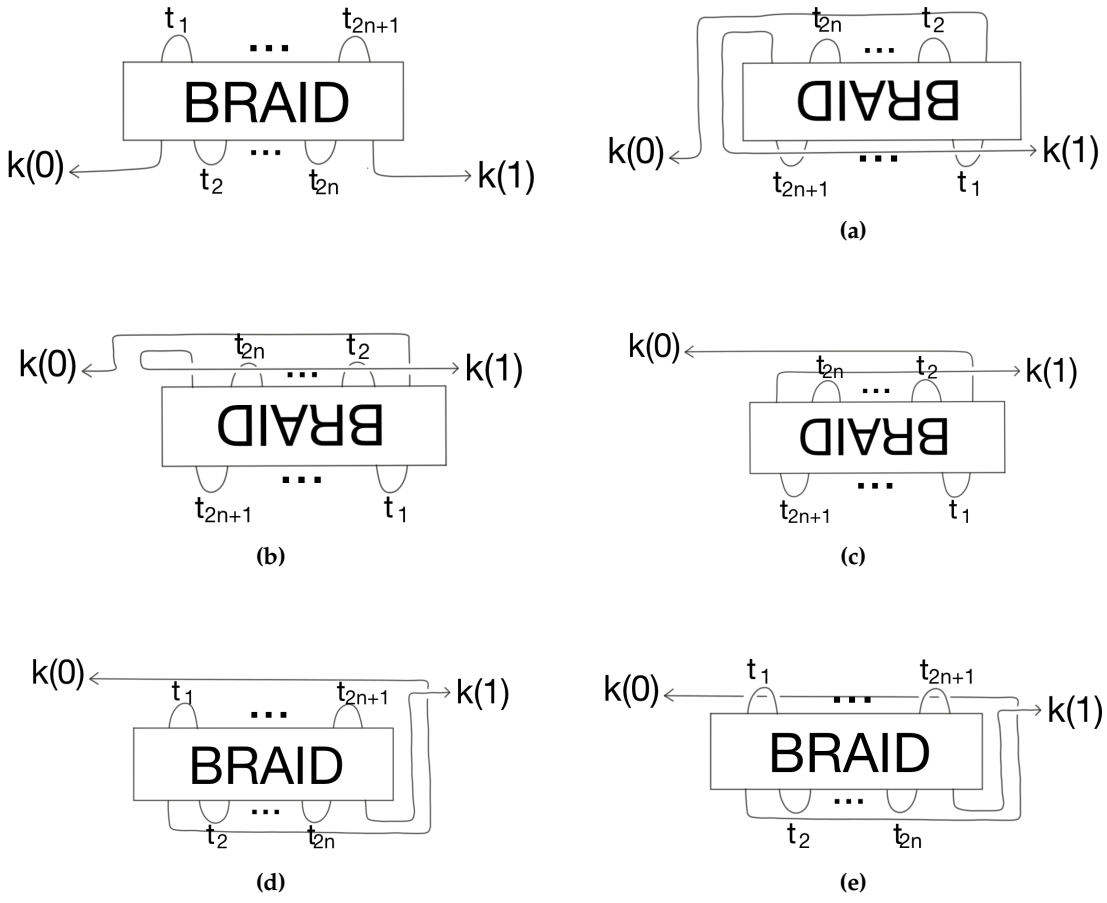

Figure 2.13 (Continued on next page): *Illustration of the stages of one full twist of k and the intersection curves of K. The y-axis points outward of the page, same as figure 2.11 but different from figure 2.12.*

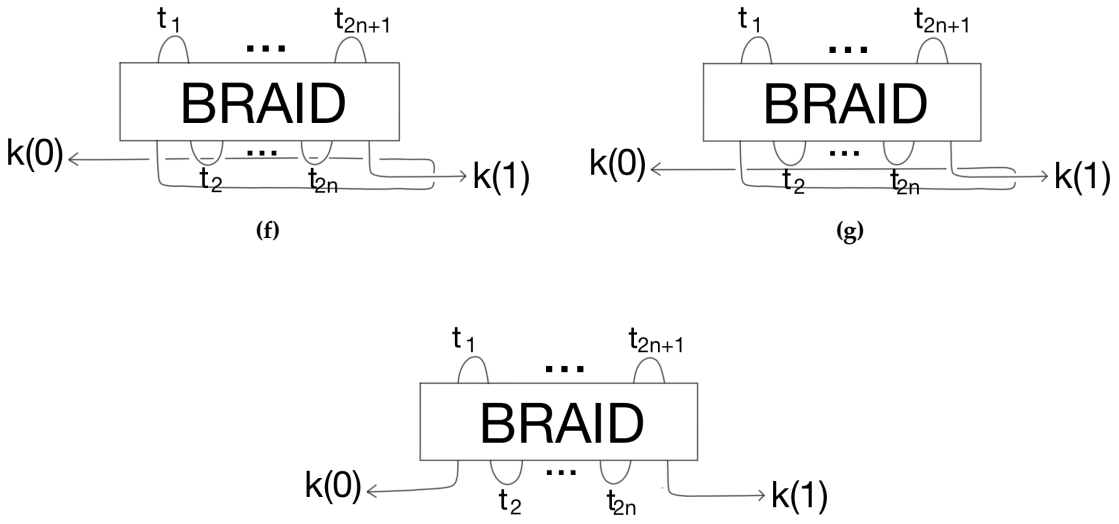

Figure 2.13 (Continued)

Figure 2.14 shows the intersection curves generated by the stages in figure 2.13.

- Originally, the intersection curves are disjoint straight curves corresponding to the crossings in the braid, arranged in the order of their t-values. The t-values t_1 through t_{2n+1} lie in between.
- Stage (a) is a collection of Reidemeister II moves. They happen at the odd numbered t-values (moving under) as well as t-values larger than t_{2n+1} (moving over). According to theorem 2.2, they generate pairs of intersection curves in cup shapes.
- Stage (b) is a sequence of Reidemeister III moves. According to theorem 2.2, the newly generated intersection curves at odd numbered t-values crosses through all the straight lines towards the even numbered t-values. The newly generated intersection curves at t-values larger than t_{2n+1} crosses through each other and copying exactly the crossing patterns of the braid in the upside-down position.
- Stage (c) is a collection of the inverse Reidemeister II moves, as well as an inverse Reidemeister I move. The intersection curves at even numbered t-values close up with each other. The intersection curves in the upside-down braid close up with each other. There is a branch point, corresponding to the inverse Reidemeister I move, produced at t

value larger than t_{2n+1}.

- Stage (d) is an isotopy in R^2 with no Reidemeister moves.
- Stages (e) is a collection of Reidemeister II moves at the odd numbered t-values (moving over) as well as t-values smaller than t_1 (moving under). The pattern of the intersection curves is similar to stage (a).
- Stages (f) is a sequence of Reidemeister III moves. The braid is upright at t-values smaller than t_1. The pattern of the intersection curves is similar to stage (b).
- Stage (g) is a collection of the inverse Reidemeister II moves. The intersection curves at even numbered t-values close up with each other. The intersection curves in the upright braid close up with each other.
- Finally, there is an inverse Reidemeister II move and an inverse Reidemeister I move. The remaining intersection curves close up accordingly, together with generating another branch point.

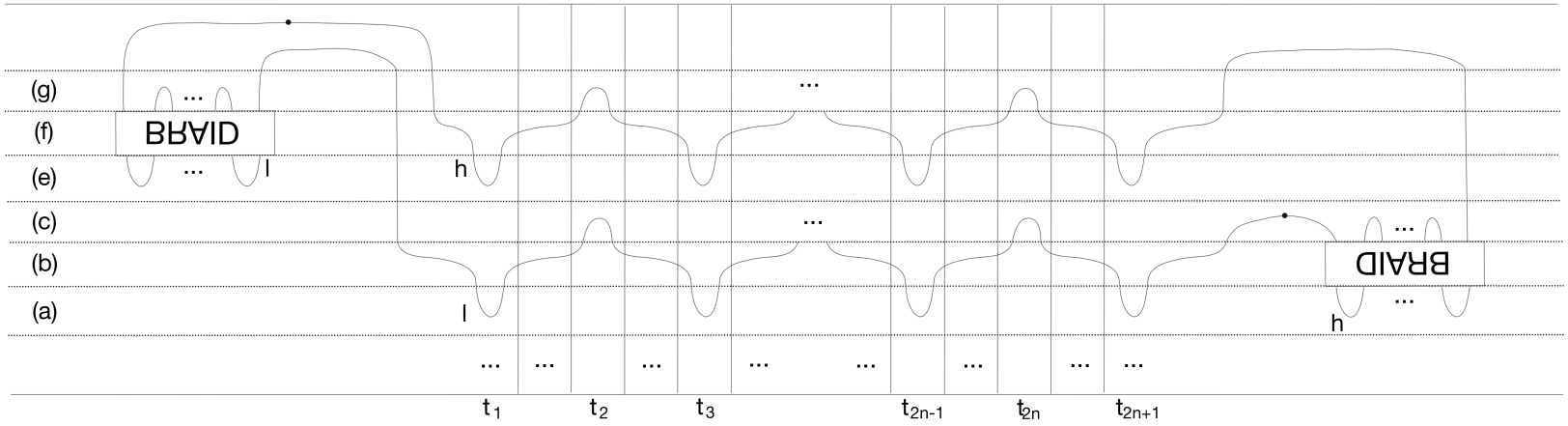

Figure 2.14: *Intersection curves of a twist spun knot, following the stages in figure 2.13.*

Chapter 3

The Roseman moves and Reidemeister moves

The Roseman moves [Ros98] of surface knots are parallel to the Reidemeister moves in knot theory. In this chapter, their effects on the intersection curves and their relations to Reidemeister moves are discussed. Let $\tau(x_1, x_2, x_3, x_4) = (x_1, x_2, x_3)$. In this chapter, regard a surface knot K as an embedding as opposed to its image. Denote the surface being embedded as S, such as S^2.

3.1 Intersection curves (h-l curves)

The intersection curves have been studied extensively in Chapter 2 in various examples. Here a formal definition is provided in general situations and additional structures are discussed.

Definition 3.1 (Intersection curves; h-l curves)**.** *The multiple point set of $\tau \circ K : S \mapsto R^3$ consists exactly of the images of n pairs of closed curves $l_i, h_i : S^1 \cong I/\partial I \mapsto S$ for $1 \leq i \leq n$; and $N-n$ pairs of open curves $l_i, h_i : I \mapsto S$ for $n+1 \leq i \leq N$.*

For all i, and all $s \in int(I)$,

$$\begin{cases} (\tau \circ K)(l_i(s)) = (\tau \circ K)(h_i(s)) \\ (x_4 \circ K)(l_i(s)) < (x_4 \circ K)(h_i(s)) \end{cases}.$$

That is, the images of an h curve in S are mapped to be higher in x_4-coordinate in R^4 by K than its partner l curve.

For $n+1 \leq i \leq N$, $l_i|_{\partial I} = h_i|_{\partial I}$ in S. Namely, each pair of the open h and l curves share endpoints. They are exactly the branch points in definition 1.4.

To avoid confusion, they are collectively named the *h-l* curves from now on (as opposed to the intersection curves in Chapter 2). In each pair, they are referred to as the partner curves of each other.

$\tau \circ K$ has finitely many triple points, exactly corresponding to the intersections among the *h-l* curves.

Theorem 3.1 (Triple point)**.** *For each triple point of $\tau \circ K$, there exist $1 \leq a, b, c \leq N$ and $\alpha, \beta, \gamma \in int(I)$ such that there are three transverse intersections of the h-l curves:*

$$\begin{cases} P_1 = l_a(\alpha) = l_b(\beta) \\ P_2 = l_c(\gamma) = h_a(\alpha) \\ P_3 = h_c(\gamma) = h_b(\beta) \end{cases}.$$

- *P_1, P_2 and P_3 map to the same image by $\tau \circ K$; and*
- *$(x_4 \circ K)(P_1) < (x_4 \circ K)(P_2) < (x_4 \circ K)(P_3)$.*

Furthermore, all the intersections among the h-l curves are transverse and uniquely grouped into these triples in one-to one correspondence to the triple points of $\tau \circ K$.

a, b and c are not required to be distinct in a triple, therefore allowing self intersections. However, they must be actual intersections. Namely, if $a = b$, then $\alpha \neq \beta$, and similarly for b, c and c, a.

As illustrated in figure 3.1(a), from the point of view of each sheet, an *h-l* curve is the shadow of another sheet passing perpendicularly. An intersection point between two

h-l curves is the shadow of the intersection line between the two perpendicular sheets. A convenient notation is therefore assigned to each intersection point, to indicate the x_4-relations of the two perpendicular, intersecting sheets whom it shadows (This is not related to the relative x_4-position of the sheet itself containing the intersection point in question).

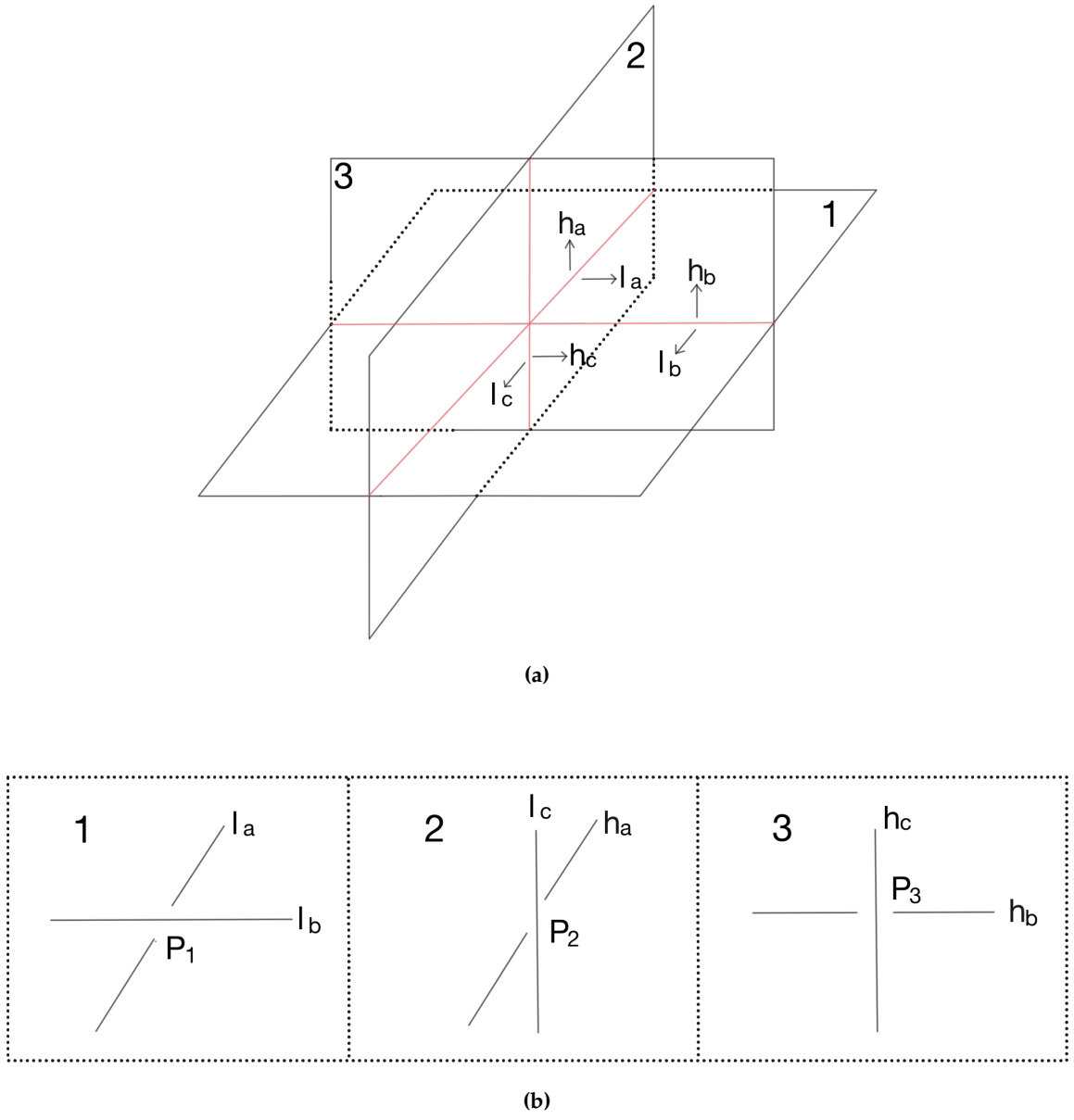

Figure 3.1: *Illustration of a triple point as a triplet of intersections among the h-l curves*

For example, in the point of view of sheet 1 (containing P_1), l_a is the shadow of sheet

2 (containing P_2) and l_b is the shadow of sheet 3 (containing P_3). Since sheet 3 has higher x_4-values than sheet 2 along the line they intersect, l_b is denoted as over l_a at P_1. This is, of course, notational only. By definition, the *h-l* curves are curves lying on the surface S and are actually intersecting (as opposed to crossing over and under) each other.

Corollary 3.2. *At each intersection between an h and an l curve, the l curve always lies over the h curve.*

Proof. By theorem 3.1, in every triple, the intersection P_2 between an h and an l curve always lies in the middle sheet among the three. In this sheet, the l curve shadows the higher sheet containing P_3 and the h curve shadows the lower sheet containing P_1. By notation, l crosses over h. □

3.2 The Roseman moves

Roseman introduced seven independent moves that cover all the equivalent cases between any surface knots [Ros98].

Theorem 3.3. *Two surface knots are equivalent if and only if they are related by a finite sequence of local Roseman moves and their inverses, along with isotopy of their projections in R^3. Figure 3.2* [Ros98, Figure 1] *defines the Roseman moves and figure 3.3* [Ros98, Figure 2] *shows the corresponding moves in the h-l curves.*

In figure 3.3, the Roseman moves are visualized by their projections in R^3 and it is assumed that the x_4-levels of the sheets in action (though not shown in the pictures) are not obstructions. This is in parallel with the description of the Reidemeister moves in figure 1.2 in Chapter 1.

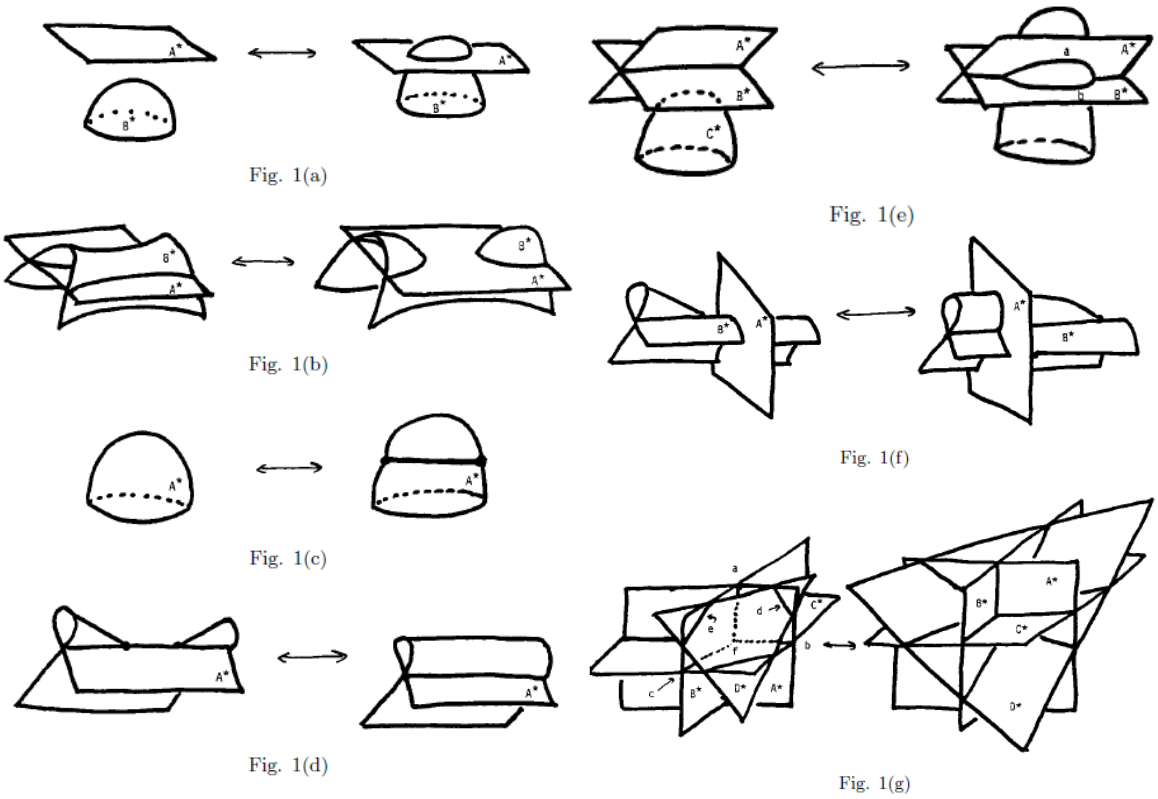

Figure 3.2: *Roseman moves projected in R^3 [Ros98, Figure 1]*

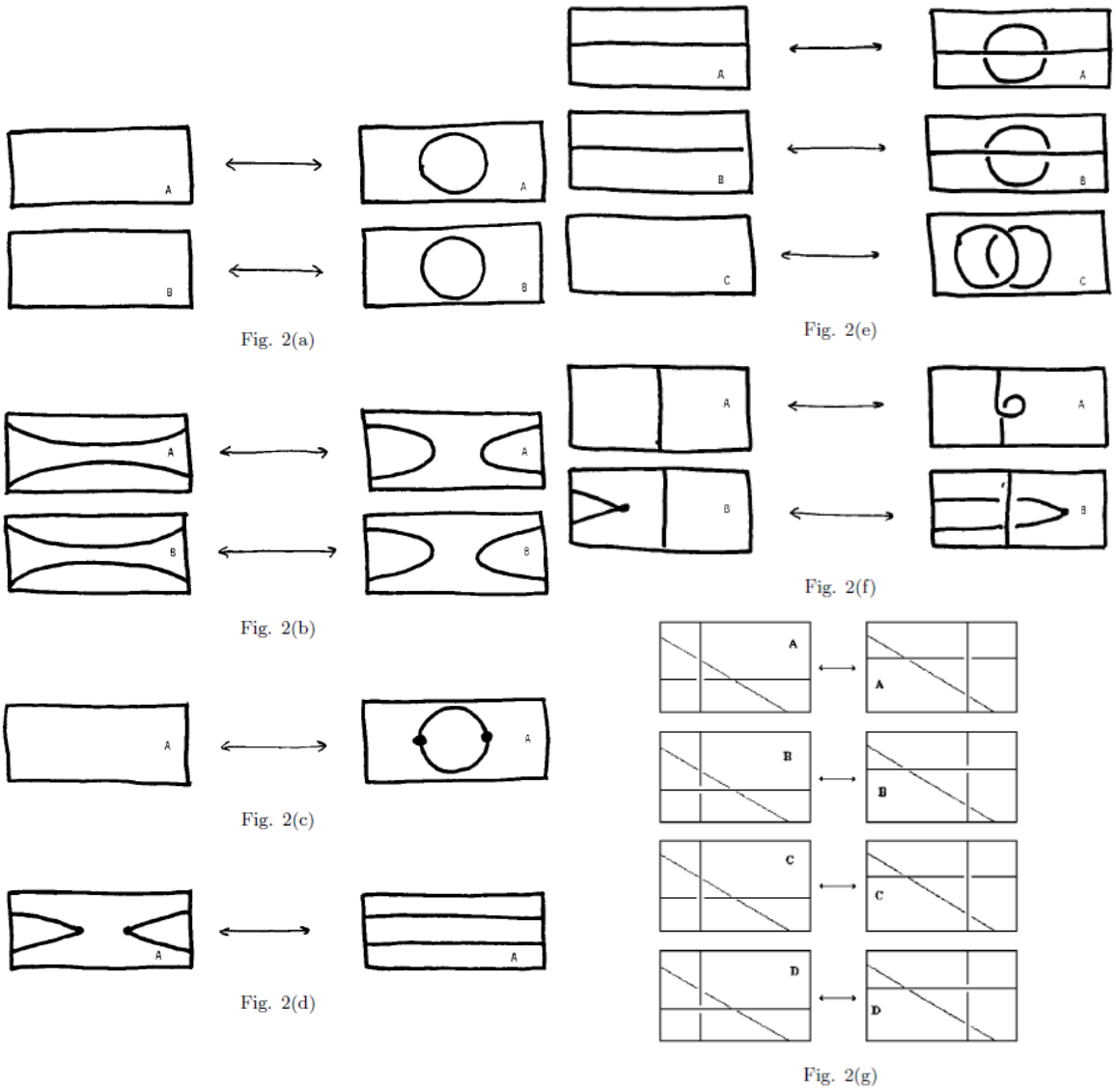

Figure 3.3: *Moves of the h-l curves due to Roseman moves [Ros98, Figure 2]*

In the sense of the over and under crossings between the *h-l* curves (according to the notation in section 3.1), the Roseman moves cannot create or break "knottings". Specifically,

- On the right side of figure 3.3 (e) and (f), in each sheet, the two crossings shadow the intersections between the same two other sheets in question, and therefore one curve must be over the other at both crossings. Namely, the two curves on each sheet must be notationally separable by a Reidemeister type II move.
- In move (g), any three of the four sheets have a common intersection in R^3. Any subset cannot have a cyclic relation in their x_4-values where each pair intersects. Equivalently, in each sheet, the move must be notationally allowable as a Reidemeister type III move.

Here is a converse statement that further observes the relationship between the Reidemeister moves on the *h-l* curves and the Roseman moves of the surface knot.

Theorem 3.4 (Reidemeister moves and Roseman moves)**.** *Any local Reidemeister move and its inverse on the h-l curves is realizable by a sequence of Roseman moves of the surface knot, at the cost of performing simultaneous Reidemeister moves on the h-l curves elsewhere.*

Proof. Figure 3.4 illustrates the procedures. Curves labelled with letters other than *h*'s and *l*'s are of arbitrary type, and the procedure works in all choices. A tilde over the same letter indicates a partner curve. Crossings without the over and under notations indicate that they depend on the curves whose types are arbitrary. The symbol $\cong$ indicates an isotopy in R^3 with no Roseman moves being performed.

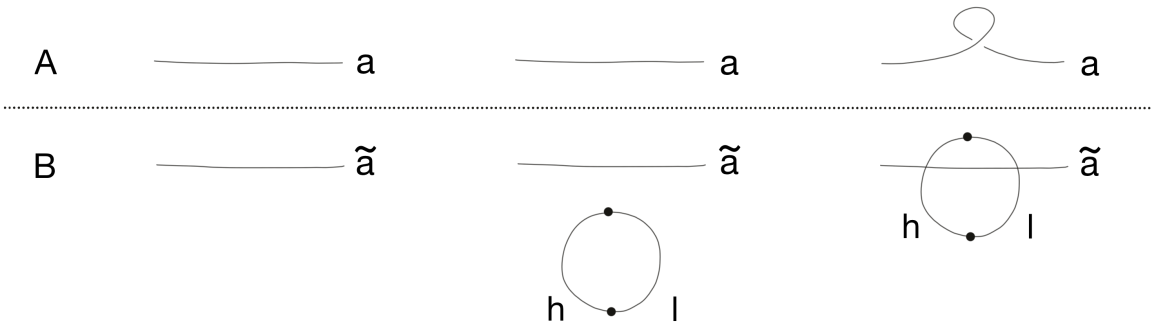

(a) *Reidemeister type I move*

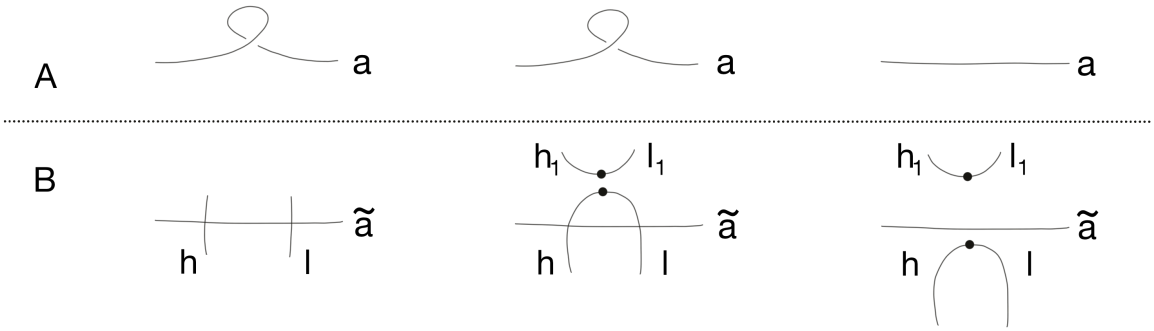

(b) *Reidemeister type I inverse move*

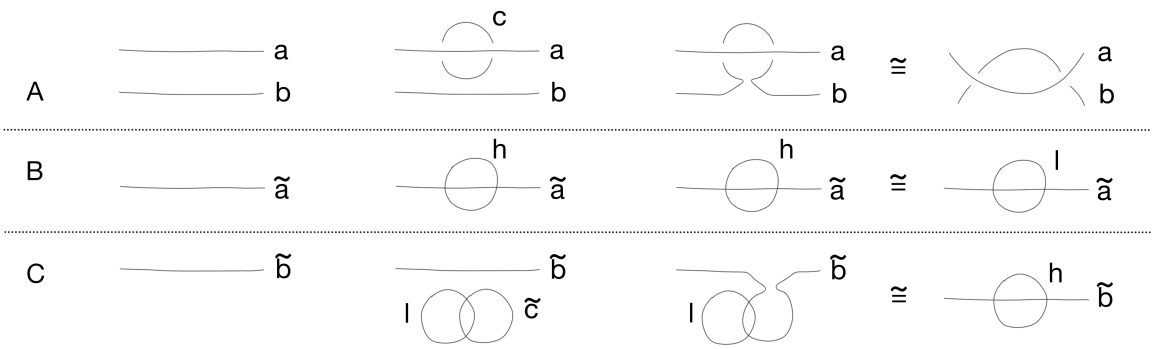

(c) *Reidemeister type II move*

Figure 3.4 (Continued on next page): *Realizations of Reidemeister moves by Roseman moves*

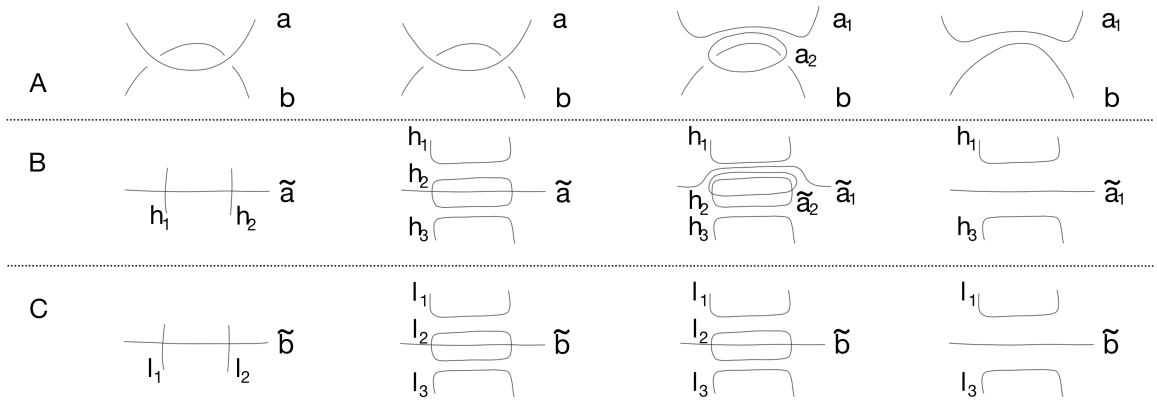

(d) *Reidemeister type II inverse move*

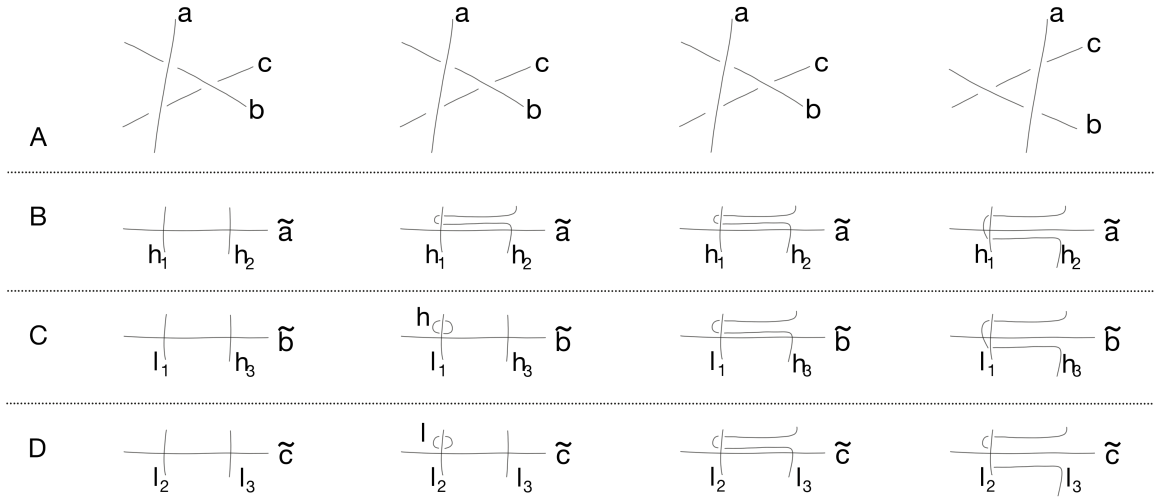

(e) *Reidemeister type III move*

Figure 3.4 (Continued)

- A Reidemeister I move is realizable by a Roseman (c) move followed by an (f) move.
- An inverse Reidemeister I move is realizable by an inverse Roseman (d) move followed by an inverse (f) move.
- A Reidemeister II move is realizable by a Roseman (e) move followed by two (b) moves. During the procedure, let the type of curve *c* be the same as curve *b*.
- An inverse Reidemeister II move is realizable by two Roseman (b) moves, followed by another (b) move only doable after the former two, and then an inverse (e) move.

Notice that the first two (b) moves are allowed only if the same types of curves are joined in sheets B and C, or equivalently, that the two crossings between a and b in sheet A are of the same type. This is equivalent to the condition that the Reidemeister II move is allowed ($\star$).

- A Reidemeister III move is covered by a Roseman (g) move if and only if all the four sheets in question and the six pairs of h-l curves perform a Reidemeister III move simultaneously. A Reidemeister II move followed by two Roseman (b) moves prepare the curves in the three other sheets. Notice the condition that the Reidemeister III move is allowed guarantees that one and only one of the two possibilities of the Reidemeister II move allows the Roseman (b) moves ($\star\star$).

($\star$) Figure 3.5(a) shows a case where the Reidemeister II inverse move is not allowed. Consequently the Roseman (b) moves are not allowed.

($\star\star$) Figure 3.5(b) shows a case where the Reidemeister III move is not allowed. By corollary 3.2, there is only one possibility for the Reidemeister II move and it prohibits the Roseman (b) moves to follow.

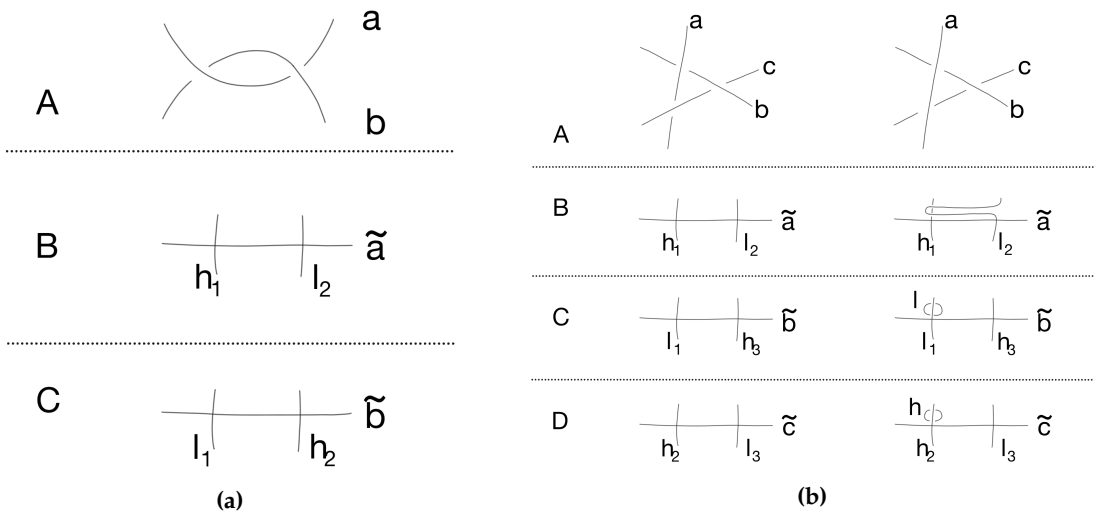

Figure 3.5: *Situations where Reidemeister moves are not allowed*

□

Chapter 4

Crossing changes and generalizations

In this chapter, attempts of generalizing the crossing changes in knot theory onto surface knots are discussed. Let $\tau(x_1, x_2, x_3, x_4) = (x_1, x_2, x_3)$. Let the surface knot be a 2-sphere: $S = S^2$.

4.1 A direct approach

4.1.1 Preliminaries

Definition 4.1. *In knot theory, a crossing change is to change the over and under relation at a particular double point in a knot diagram, thus possibly changing the knot diagram to represent a different knot than the original.*

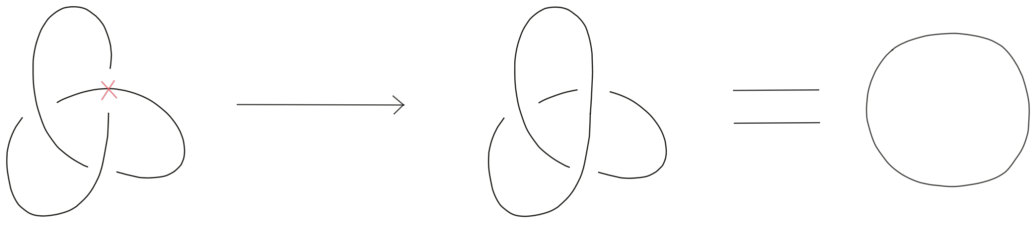

Figure 4.1: *A crossing change on a knot diagram of the trefoil knot (figure 1.1) at the double point marked by red, resulting in a knot diagram that represents the trivial knot*

Figure 4.1 is an example of a crossing change. A natural generalization of the crossing

change onto a surface knot is to switch the roles of a particular pair of the *h*-*l* curves (denoted h_0 and l_0 from now on) by lifting the x_4-value in a regular neighborhood of the l_0 curve such that it becomes pointwisely higher than the original h_0 curve. (Equivalently, this can also be achieved by lowering the x_4-value in a regular neighborhood of the original h_0 curve.) The procedure should be performed only in the x_4-dimension and keep the projection $\tau \circ K$ fixed, same as in the knot diagram situation.

Since the procedure does not change the projection $\tau \circ K$, the *h*-*l* curves are unchanged in S.

The aforementioned crossing change has no obstructions except possibly at the intersections of h_0 or l_0 with any *h*-*l* curves (including self-intersections). According to theorem 3.1, all the intersections between *h*-*l* curves are grouped into triples such that, in each triple, there is exactly one intersection between two *h* curves, two *l* curves, and one *h* and one *l* curve, respectively. Conceptually, this is because the three sheets at a triple point have a consistent ordering of x_4-values along their mutual intersections, as shown in figure 3.1.

Theorem 4.1. *The following statements are equivalent:*

1. *The aforementioned crossing change can be performed on the pair of curves h_0 and l_0.*
2. *At all triple points of $\tau \circ K$ that are associated with h_0 and l_0, the crossing change results in a consistent reordering of x_4 of the three sheets.*
3. *After switching the names of h_0 and l_0, there does not exist a triple of intersections among the h-l curves where all the three intersections are between an h and an l curve.*

The proof is straightforward. By the third statement, the question whether a crossing change is permitted has a combinatorial nature.

Here are two examples. In figure 4.2, the crossing change is not allowed since it results in three intersections between *h* curves and *l* curves afterwards. Conceptually, this is attempting to change the x_4-ordering between the highest sheet (sheet 1) and the lowest sheet (sheet 3) at a triple point. Therefore the middle sheet becomes an obstruction.

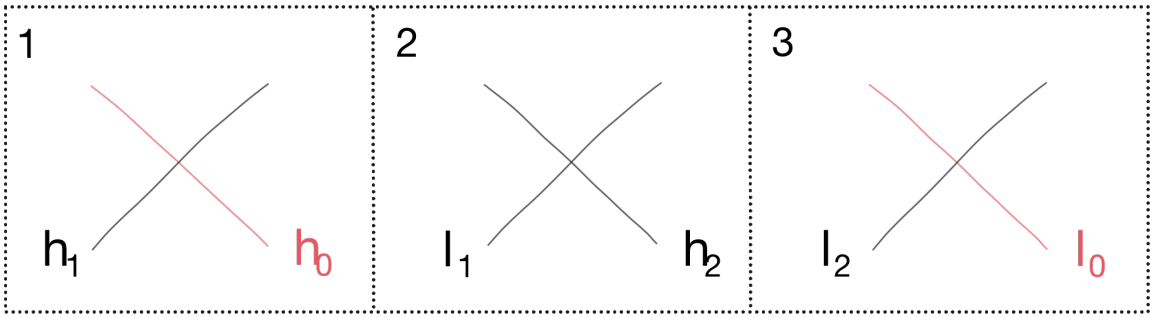

(a) *Before crossing change between h_0 and l_0*

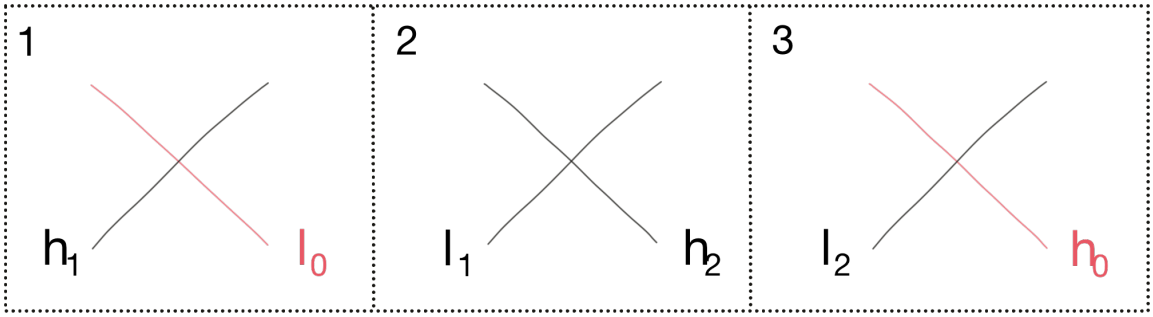

(b) *After attempted crossing change, resulting in a unrealistic situation*

Figure 4.2: *An examples of triple points allowing or obstructing a crossing change between h_0 and l_0*

In figure 4.3, the crossing change is allowed. This is an example with a self-intersection of h_0. Conceptually, at the triple point the highest sheet (sheet 1) becomes the lowest after the change and the middle and lowest sheets (sheets 2 and 3, respectively) becomes the highest and middle sheets. The ordering is consistent and there is no obstruction.

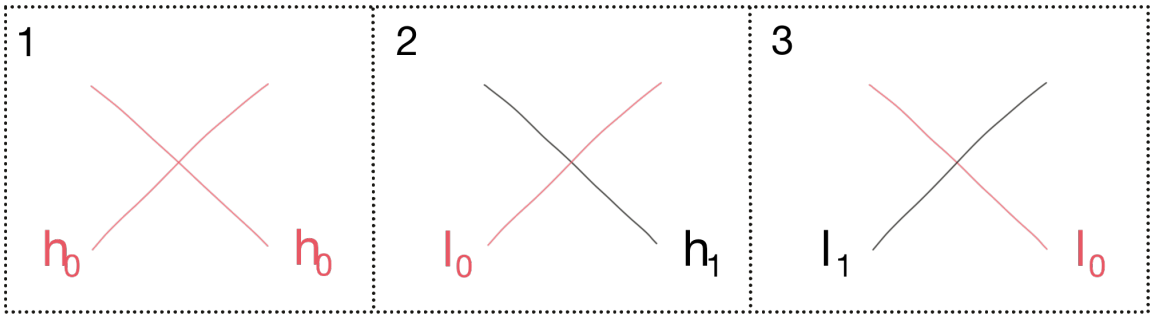

(a) *Before crossing change between h_0 and l_0*

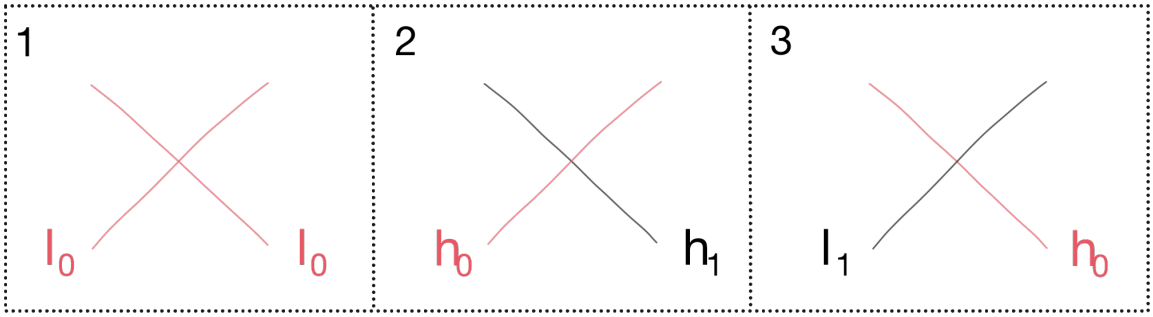

(b) *After the crossing change*

Figure 4.3: *Another example of triple points allowing or obstructing a crossing change between h_0 and l_0*

To fully generalize the crossing change, one possible way is to do a crossing change on any obstructing curves simultaneously. In figure 4.2 above the crossing change is not allowed. If a crossing change is simultaneously performed on h_1 and l_1, however, then it becomes allowed. See figure 4.4.

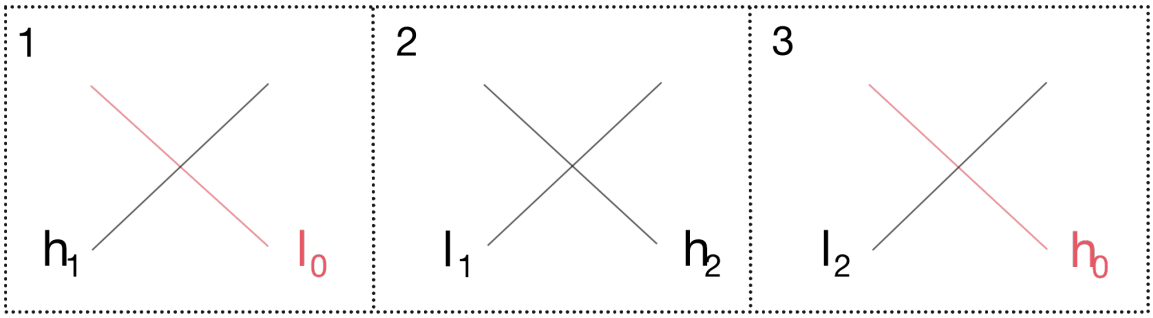

(a) *The prohibited configuration (figure 4.2(b)) after the proposed crossing change*

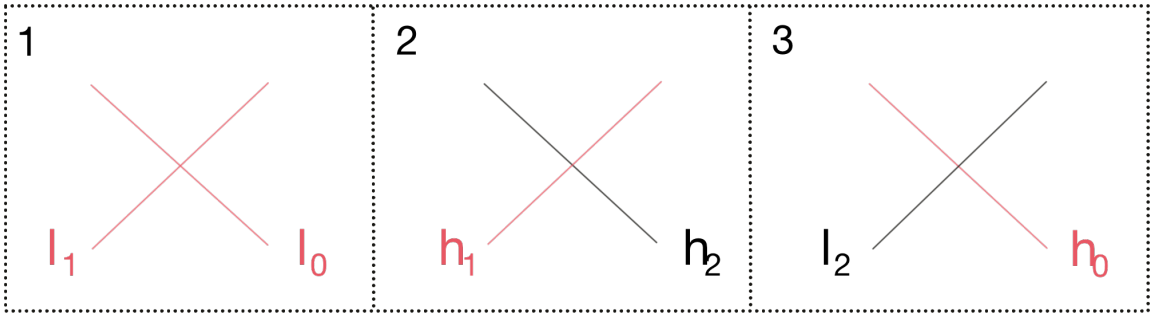

(b) *After performing a crossing change between h_1 and l_1 simultaneously*

Figure 4.4: *A chain reaction of crossing changes*

It can be shown that this eventually leads to doing crossing changes on a subset of all the *h-l* pairs. In the later sections, other methods of generalizing the crossing changes are explored.

4.1.2 An example of the chain reaction of crossing changes

In this subsection, the 2-twist spun trefoil knot is presented as an example of the chain reaction of crossing changes.

In subsection 2.3.2, the general structure of the *h-l* curves of any twist spun knot is constructed, based on a standard procedure of twisting a knot in R^3 in braid configuration. A different sequence of Reidemeister moves may also twist the knot, and produce the equivalent twist spun knot with a different (non-standard but possibly simpler) set of *h-l*

curves. Figure 4.5 shows a sequence of Reidemeister moves that turns the trefoil knot halfway through a full twist.

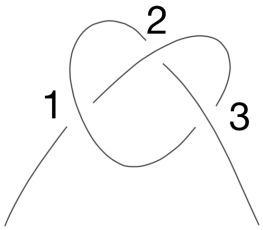

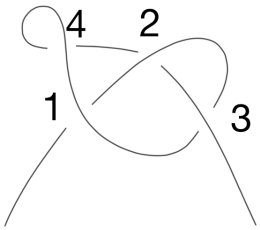

(a) *Type I at 4*

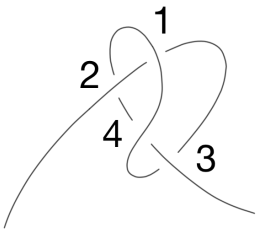

(b) *Type III at 1,2,4*

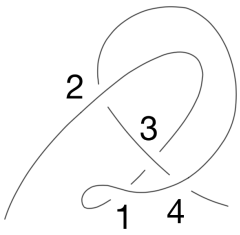

(c) *Type III at 1,3,4*

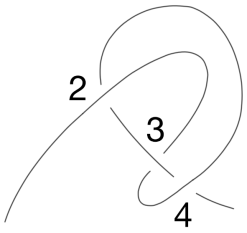

(d) *Type I inverse at 1*

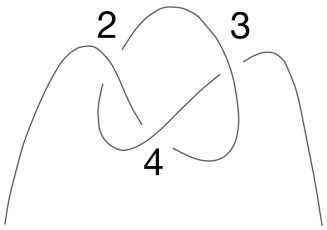

Figure 4.5: *A sequence of Reidemeister moves that turns the trefoil knot over*

By theorem 2.2, the *h-l* curves are constructed in figure 4.6. The later half of the twist is a copy of the former half, starting with the new set of curves (numbered 2,3,4) after the first half.

In figure 4.6, the *h-l* curves are numbered consistently with the double points in the knot diagram in figure 4.5. As *h-l* curves, however, the three pairs of curves numbered 1,3,5 are the same pair, connected through the top and bottom of the parametrization space, despite their different numbers. In this subsection, denote such equivalence of numbers by 1=3=5.

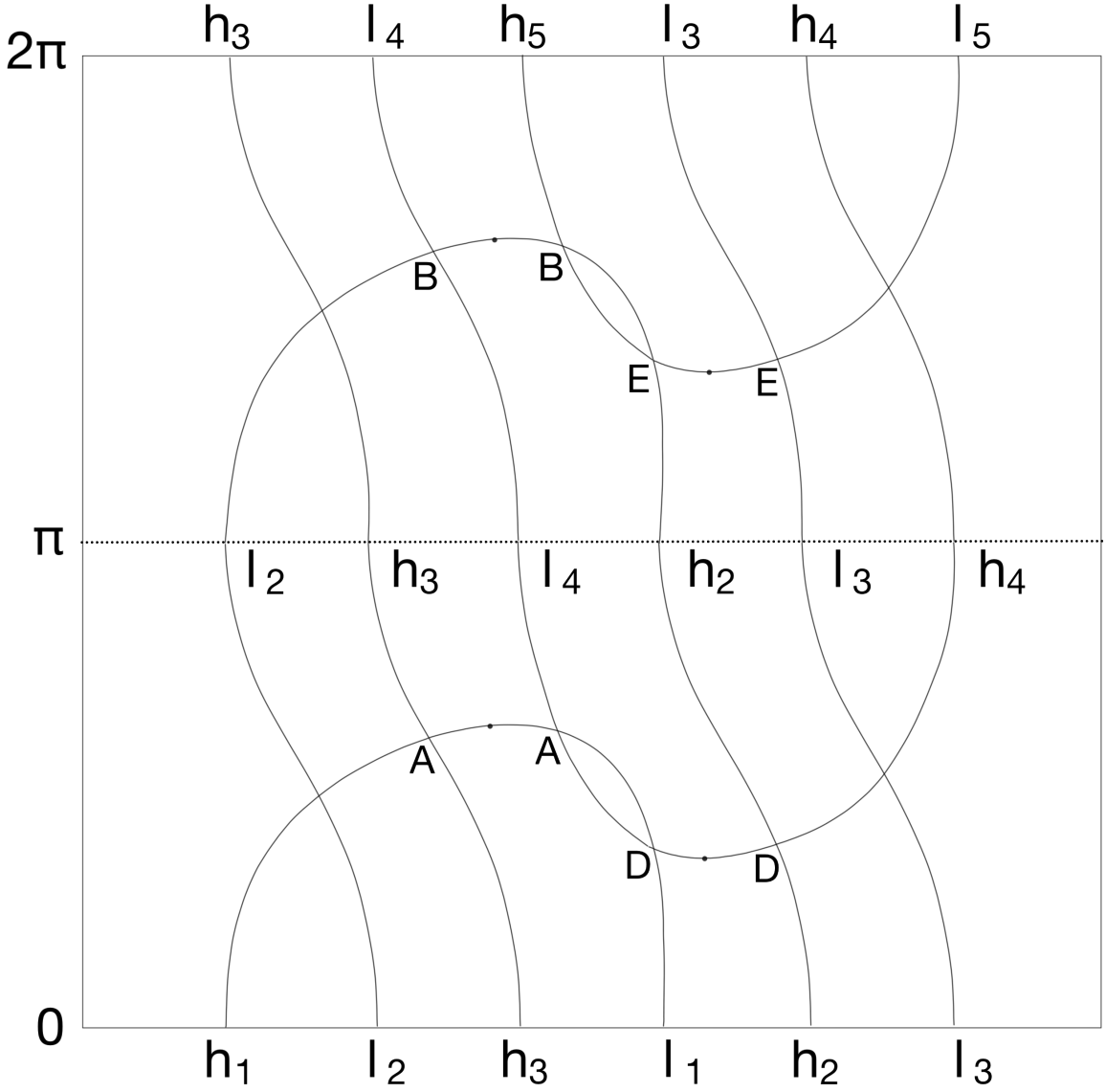

Figure 4.6: *The h-l curves of the 1-twist spun trefoil knot*

Similarly, 2=4.

The points marked with A through E in figure 4.6 are obstruction points to crossing changes.

- The A points obstruct the crossing change between h_1 and l_1. In order to do this crossing change, the pair of curves 3 or 4 must change simultaneously. According to figure 4.4, releasing the obstruction at either one of a pair of obstruction points suffices to allow the crossing change.
- The B points obstruct the crossing change between h_2 and l_2. The pair of curves 4 or 5 must change simultaneously.
- The D points obstruct the crossing change between h_4 and l_4. The pair of curves 1 or 2 must change simultaneously.
- The E points obstruct the crossing change between h_5 and l_5. The pair of curves 2 or 3 must change simultaneously.

Combining with the fact that there are only two different pairs of curves, 1=3=5 and 2=4, there is no obstruction to performing a crossing change on either pair alone.

For the 2-twist spun trefoil knot, the *h-l* curves picture is two copies of figure 4.6 stacked on top of each other. The second copy starts with the set of curves numbered $3, 4, 5$ and ends with $5, 6, 7$, in parallel to the first copy.

The new equivalences between the numbers of the curves are 1=5, 2=6 and 3=7, connected from the top (of the second copy) to the bottom (of the fist copy) of the parametrization space. There are four pairs of curves.

In addition to the above four obstruction rules, there are four more. Table 4.1 summarizes the obstructions to the crossing changes between each pair of curves. The second row is a summary of the discussions above, and the third row reasonably resembles the second row by replacing 1 through 5 by 3 through 7. In each element, the two numbers indicate that performing a crossing change on either number suffices to allow the crossing change in the first row.

Table 4.1: *Crossing change obstruction information for 2-twist spun trefoil knot*

Crossing change	1	2	3	4	5	6	7
Obstruction (1st twist)	3, 4	4, 5		1, 2	2, 3		
Obstruction (2nd twist)			5, 6	6, 7		3, 4	4, 5

Combining with the equivalences of the numbers of the curves, the conclusion is that a crossing change is not possible between any pair of *h-l* curves alone. In this example, at least two or more pairs must be changed. For example, simultaneous crossing changes between the two pairs 1=5 and 3=7 is allowed. So are the simultaneous changes between 2=6 and 4.

4.2 The disjoint simple-closed case

In this section, let h_0 and l_0 be disjoint simple closed curves. Though this is a special case, it is very common in various examples, as shown in Chapter 2.

4.2.1 Arguments in R^4

Assume for now that h_0 and l_0 bound disjoint discs $D_h, D_l \cong D^2$ in S. This is automatically true if $S = S^2$. Assume further that the $\tau \circ K|_{int(D_h \cup D_l)}$ is an embedding in R^3.

Define the subset $S_0 = K(D_h) \cup K(D_l) \cup C_0 \subset R^4$ where C_0 is the "vertical" cylinder (i.e., parallel to the x_4-axis) between the boundaries of $K(D_h)$ and $K(D_l)$: $C_0 = \bigsqcup_{t \in S^1} \{\tau \circ K(l_0(t))\} \times [x_4 \circ K(l_0(t)), x_4 \circ K(h_0(t))]$. $S_0 \cong S^2$. $\tau(S_0) = \tau \circ K(D_h \cup D_l)$ is by assumption an embedded S^2 in R^3. Therefore, S_0 is a trivially embedded S^2 in R^4. Let it bound a 3-ball B_0 in R^4.

In general position in the 4-dimensional space R^4, the 3-dimensional B_0 intersects the 2-dimensional $K(S - (D_h \cup D_l))$ in a subset L_0 which is the union of 1-dimensional disjoint

simple curves. $L_0 = B_0 \cap K(S - (D_h \cup D_l))$. Since K is injective, L_0 intersects $S_0 = \partial B_0$ in C_0. There exists a larger 3-ball $\tilde{B_0} \supset B_0$ in R^4 and an isotopy $F : \tilde{B_0} \times [0,1] \mapsto \tilde{B_0}$ such that

- F is compactly supported in $\tilde{B_0}$, i.e., $F(\cdot, s)|_{\partial \tilde{B_0}} = id_{\partial \tilde{B_0}}$ for all s;
- $F(\cdot, s)|_{K(D_h \cup D_l)} = id_{K(D_h \cup D_l)}$ for all s; and
- $F(L_0, 1) \subset \tilde{B_0} - B_0$.

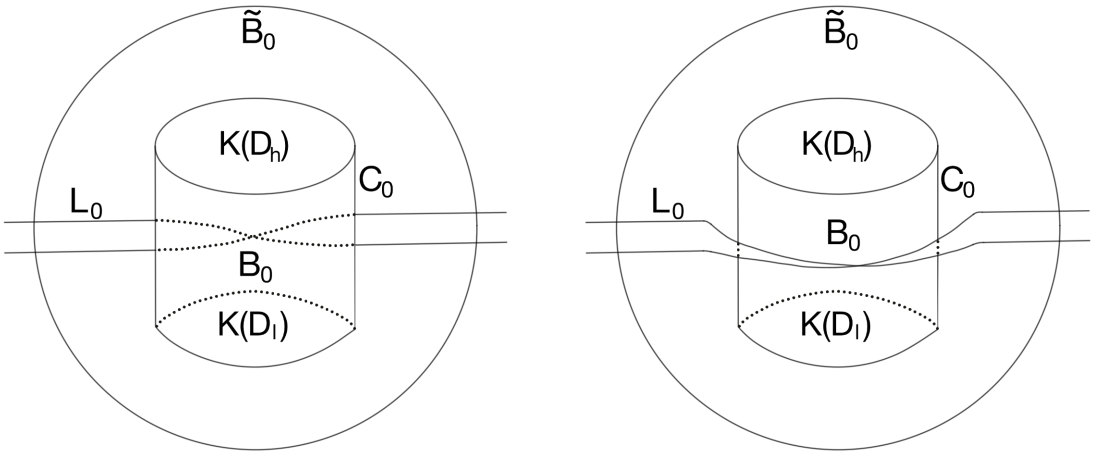

(a) *Before the isotopy* **(b)** *After the isotopy*

Figure 4.7: *An illustration of the ambient isotopy in the 3-ball $\tilde{B_0}$*

Conceptually, this is an ambient isotopy that pulls the union L_0 of the disjoint simple curves out from B_0 via C_0, without intersecting $K(D_h \cup D_l)$ along the process. In figure 4.7, L_0 schematically represents a collection of disjoint simple curves, whose internal structure is not shown.

This ambient isotopy can be extended to an isotopy of the embedding K of S in R^4. Since $L_0 \subset K(S - (D_h \cup D_l))$, consider a regular neighborhood $N_0 \subset S$ of its preimage $K^{-1}(L_0)$ such that $N_0 \cap (D_h \cup D_l) = \emptyset$. Let N_0 be parametrized by the homeomorphism $N_0 \cong L_0 \times [-1, 1]$. Define the new embedding $\tilde{K}$.

$$\tilde{K}(x) = \begin{cases} K(x) & \text{for } x \in S - N_0 \\ F(p, 1 - |s|) & \text{for } x = \{p, s\} \in L_0 \times [-1, 1] \cong N_0 \end{cases}.$$

After smoothing the corners, the new embedding $\tilde{K}$ is ambient isotopic in R^4 (i.e., equivalent) to the original surface knot K and is identical to K in $D_h \cup D_l$. $B_0 \cap \tilde{K}(S - (D_h \cup D_l)) = \emptyset$. This suggests that at all the triple points of $\tau \circ \tilde{K}$ on $\tau \circ \tilde{K}(h_0) = \tau \circ \tilde{K}(l_0)$, the third sheet lies, in the x_4-level, either above or below both $\tau \circ \tilde{K}(D_h)$ and $\tau \circ \tilde{K}(D_l)$, but can never be in the middle. The crossing change can then be performed without obstructions.

In fact, the requirement of the existence of the 3-ball B_0 is stronger than necessary. For the construction of the ambient isotopy F, it is sufficient to require the existence of a solid cylinder whose side is a subset of C_0.

4.2.2 The *h-l* curves

In this subsection, a detailed survey of L_0 is presented by switching the viewpoint to the image of $\tau \circ K$ in R^3. Furthermore, examples are constructed to discuss the effects on the *h-l* curves caused by the modification of the surface knot from K to $\tilde{K}$.

The obstructions to the crossing change between h_0 and l_0 are the triple points of $\tau \circ K$ on $\tau \circ K(h_0) = \tau \circ K(l_0)$ where the third sheet lies in the middle, in x_4-levels, between the two sheets $\tau \circ K(D_h)$ and $\tau \circ K(D_l)$.

For $1 \leq i \leq n$, let $t_i \in S^1$ be all the positions on h_0 such that an *h-l* curve a_i intersects h_0 at $h_0(t_i)$. According to theorem 3.1, there is an *h-l* curve b_i intersecting l_0 at $l_0(t_i)$. Further more, $\tilde{a_i}$ and $\tilde{b_i}$ intersect at $x_i \in S - (D_h \cup D_l)$, where a tilde indicates a partner curve. See figure 4.8.

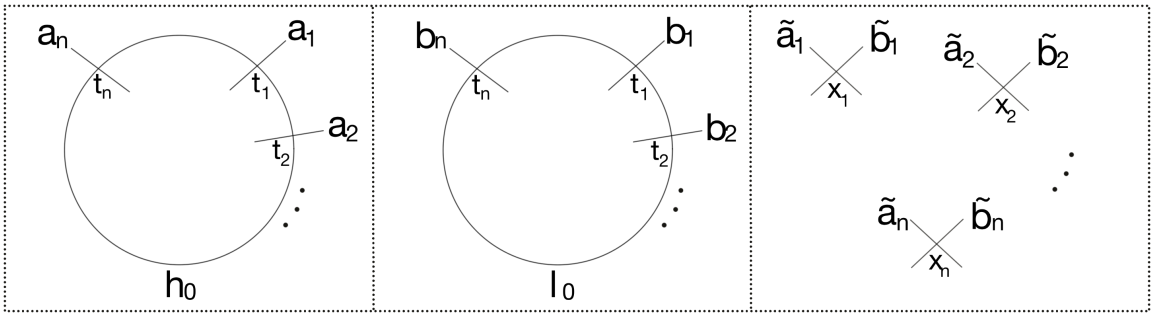

Figure 4.8: *The intersections of h_0 and l_0 with other h-l curves*

Since D_h is a disc in S, the collection of points $\{h(t_i)\}$ are pairwisely connected by the collection of curves $\{a_i\}$ inside D_h. Namely, for each p, there exists a unique $q \neq p$ such that a_p and a_q are the same curve connecting $h(t_p)$ and $h(t_q)$ inside D_h. Same for l_0 and the b_i's.

The obstructions to the crossing change are exactly the t_i's where a_i is an h curve and b_i is an l curve (theorem 4.1).

Theorem 4.2. *The obstruction points on h_0 and l_0 can be grouped into pairs such that there exist mutually disjoint curves in $int(\tau(B_0)) \cap \tau \circ K(S - (D_h \cup D_l))$ connecting each pair.*

Proof. Pick an arbitrary obstruction point t_{i_0}. Namely, a_{i_0} is an h curve and b_{i_0} is an l curve. Enter the following algorithm with the current index $p = 0$ and an ordered list with current value $I = \{i_0\}$.

1. There exists a unique i_{p+1} such that $h(t_{i_p})$ is connected with $h(t_{i_{p+1}})$ in D_h, by the curve a_{i_p} which is the same curve as $a_{i_{p+1}}$. $a_{i_{p+1}}$ is therefore an h curve. Add i_{p+1} to the list I.
2. If $b_{i_{p+1}}$ is an l curve, exit the algorithm.

   Otherwise, $b_{i_{p+1}}$ is an h curve. There exists a unique i_{p+2} such that $l(t_{i_{p+1}})$ is connected with $l(t_{i_{p+2}})$ in D_l, by the curve $b_{i_{p+1}}$ which is the same curve as $b_{i_{p+2}}$. $b_{i_{p+2}}$ is therefore an h curve. Add i_{p+2} to the list I.
3. Since $b_{i_{p+2}}$ is an h curve which intersects l_0, $a_{i_{p+2}}$ cannot be an l curve which intersects h_0 (theorem 3.1). $a_{i_{p+2}}$ is therefore an h curve. Update p to be $p + 2$ and go back to Step 1.

Several properties follow from the construction.

- Since the total number of intersection points is finite, the algorithm ends after finitely many steps. Furthermore, at each time back at Step 1, p is an even number. Therefore, the last element in I has an odd subscript (call it i_m) and I contains an even number of elements (including i_0). For any given i_0, I is uniquely generated.
- I contains distinct elements, and especially, $i_m \neq i_0$. Aside from i_0 and i_m, I contains a sequence of subscripts of non-obstruction points. By construction, for all $i_p \in I - \{i_0, i_m\}$, both a_{i_p} and b_{i_p} are h curves and t_{i_p} is not an obstruction point. If the algorithm starts

from i_m, then I is generated exactly reversely. Any two lists generated by the algorithm are either the same (or the reverse of each other) or completely disjoint.

- There exists a piecewise curve $c(i_0, i_m)$ in $S - (D_h \cup D_l)$ passing through the collection of points $\{x_{i_p}\}$ for all $i_p \in I$ in order, by following $\tilde{a_{i_p}}$ from x_{i_p} to $x_{i_{p+1}}$ for even p, and $\tilde{b_{i_p}}$ for odd p, alternately. $\tau \circ K(c(i_0, i_m)) \subset \tau(S_0)$, with segments lying in $\tau \circ K(D_h)$ and $\tau \circ K(D_l)$ alternately.

Therefore, all the obstruction points are grouped uniquely into pairs. Slightly perturb all the curves in $S - (D_h \cup D_l)$ ensures that their images lie in $int(B_0)$ and are mutually disjoint. □

Figure 4.9 illustrates the process using an example with only one pair of obstruction points. The rightmost points on h_0 and l_0 are their respective intersections with h_3 and l_6, and the leftmost points on h_0 and l_0 are the intersections with h_1 and l_4. The algorithm goes through Step 1 twice and exits at the second time in Step 2. The sequence I contains 4 points (an even number) and the curve $c(i_0, i_m)$ contains 3 segments.

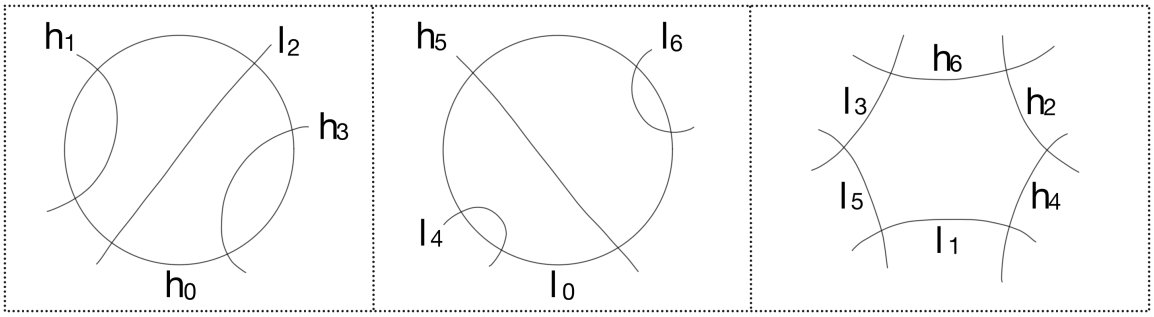

(a) *An example with a single pair of obstruction points*

Figure 4.9 (Continued on next page): *An example of the algorithm in theorem 4.2 and the curve generated*

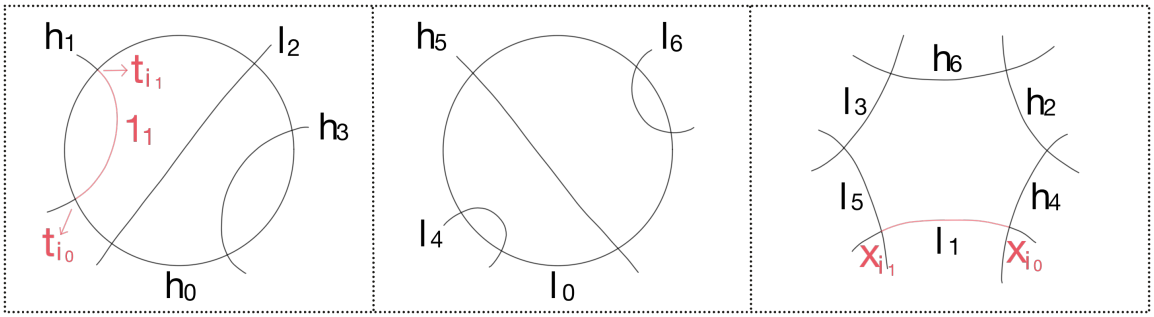

(b) *Step 1*

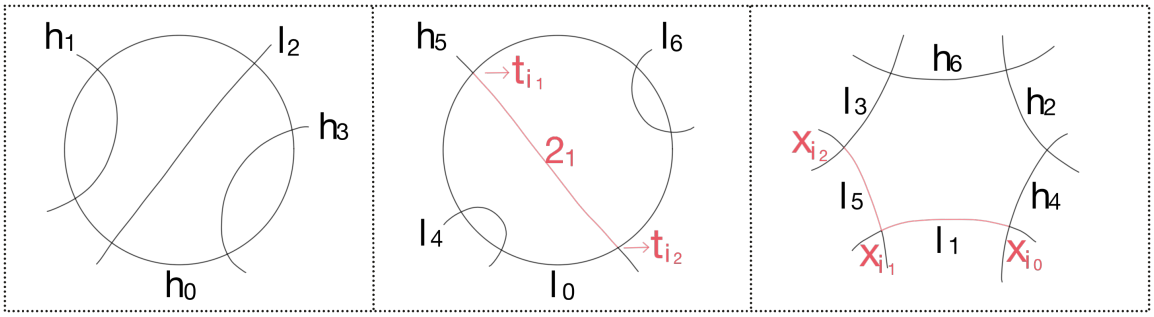

(c) *Step 2 (not exiting)*

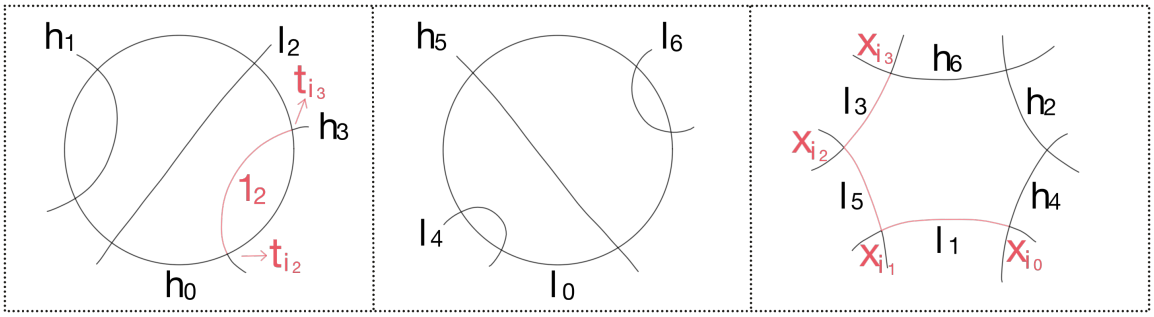

(d) *Step 1, second time*

Figure 4.9 (Continued)

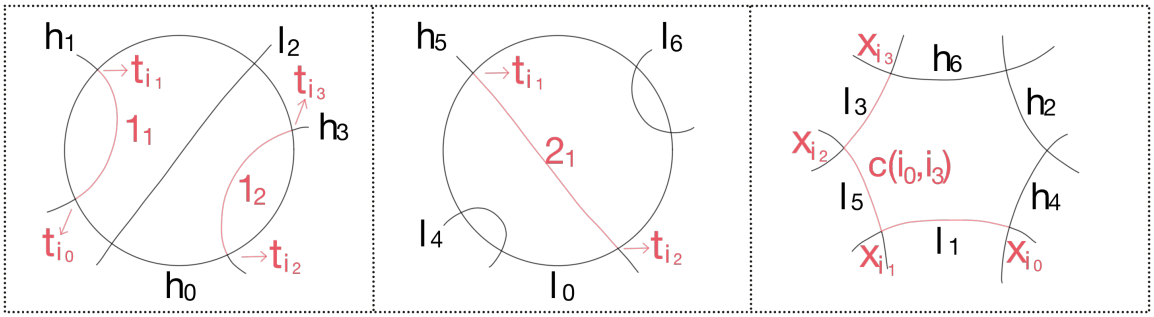

(e) *The final sequence I and curve $c(i_0, i_m)$*

Figure 4.9 (Continued)

$\tau(S_0)$ bounds a unique 3-ball in R^3, equal to $\tau(B_0)$. B_0 is any of its lift in R^4 and is not unique. Depending on the choice of B_0, the collection of curves $\tau \circ K(\{c(i_0, i_m)\})$ can be the projection $\tau(L_0)$ in R^3.

Each non-obstruction point that the sequence I contains (i.e., each element in I aside from the first and the last) causes a twist in the band. Figure 4.10 illustrates the correspondence of a twist and a passing element in I using an unrealistic model of an I containing 3 elements (an odd number). In figure 4.10(a), $\tau \circ K(c(i_0, i_m))$ passes near one point on $\tau \circ K(h_0) = \tau \circ K(l_0)$ along its way, and contains two segments near $\tau \circ K(D_h)$ and $\tau \circ K(D_l)$ respectively. It is isotopic to the band with one twist in figure 4.10(b). Therefore, theorem 4.2 shows that a regular neighborhood of each curve $\tau \circ K(c(i_0, i_m))$ in $\tau \circ K(S)$ is a band passing through $\tau(B_0)$ with an even number of twists.

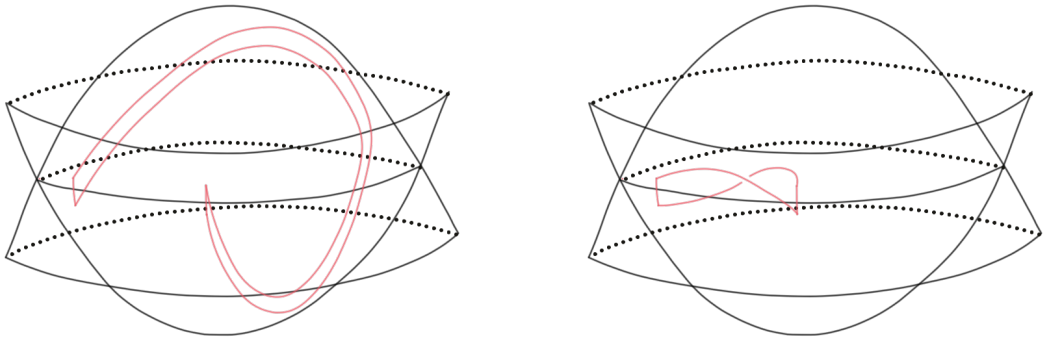

(a) $\tau \circ K(c(i_0, i_m))$ *with one passing point*

(b) *An isotopic band*

Figure 4.10: *Illustration of the correspondence between the number of elements in I and the number of twists in a band neighborhood of* $\tau \circ K(c(i_0, i_m))$.

Finally, two examples are presented to illustrate the effects on the *h-l* curves after the modification of the surface knot K to $\tilde{K}$ in R^4. The examples are done with only one band in each picture (the red band) to be pulled out by isotopy. Figure 4.11 shows the basic (zero-twist) case.

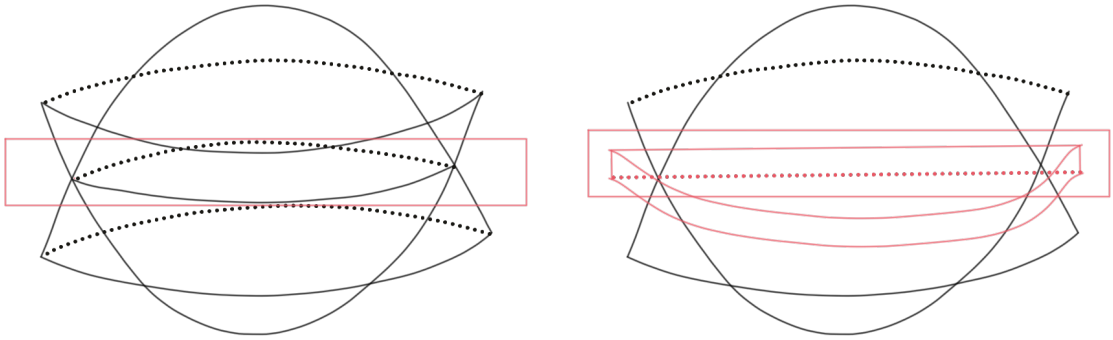

(a) *Parts of* $\tau \circ K(S)$ *in* R^3

(b) *Parts of* $\tau \circ \tilde{K}(S)$ *in* R^3

Figure 4.11 (Continued on next page): *An example of the zero-twist band*

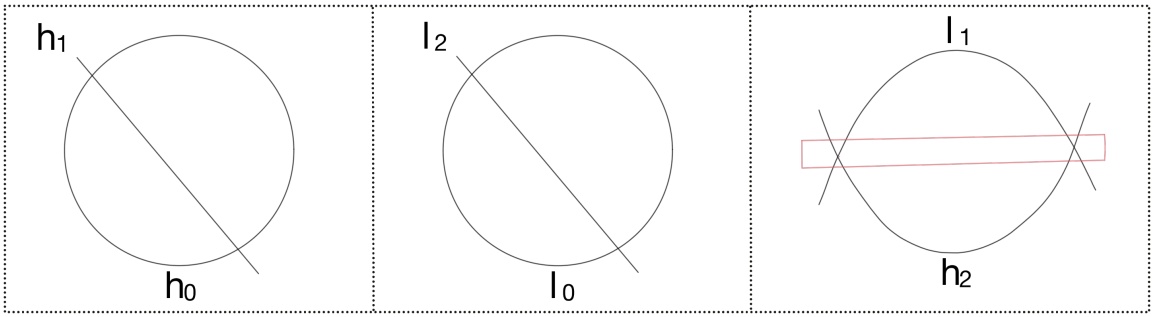

(c) *The relevant h-l curves of K*

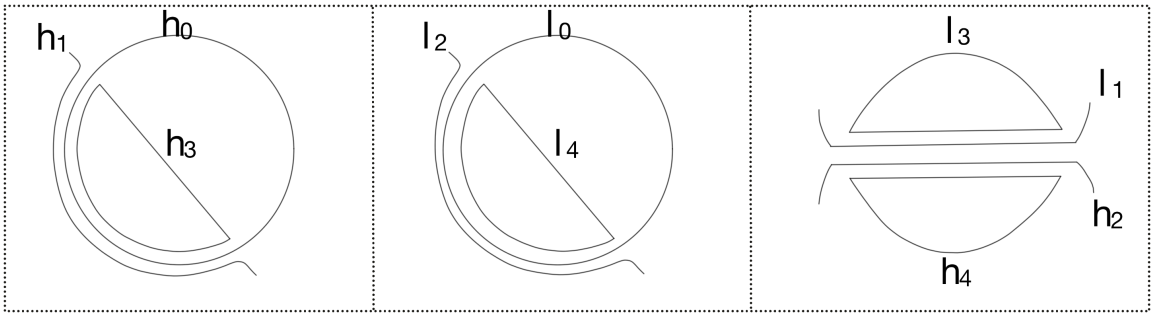

(d) *The relevant h-l curves of* $\tilde{K}$

Figure 4.11 (Continued)

Figure 4.12 shows an example of a single two-twist band case (the same example studied in figure 4.9). The trace of each twist is a Whitney umbrella in R^3. Therefore, there are two pairs of branch points generated in the *h-l* curves of $\tilde{K}$.

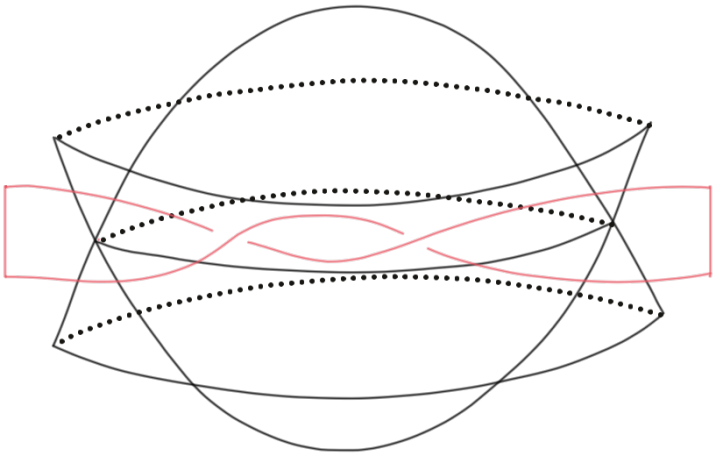

(a) *Parts of $\tau \circ K(S)$ in R^3*

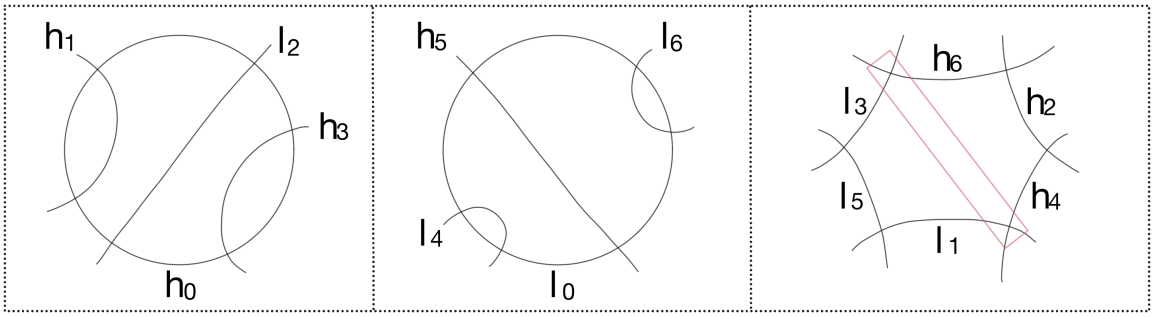

(b) *The relevant h-l curves of K*

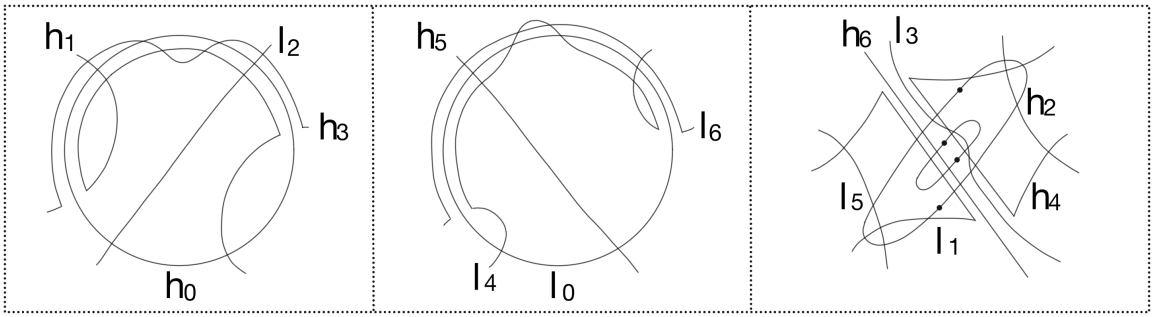

(c) *The relevant h-l curves of $\tilde{K}$*

Figure 4.12: *An example of a two-twist band as in figure 4.9*

4.3 The simple closed case

As a corollary of corollary 3.2 and theorem 3.4, there is the following claim:

Corollary 4.3. *Simple closed h_0 and l_0 are essentially disjoint after a sequence of Roseman moves.*

Proof. The proof is straightforward, noticing the following facts.

- By corollary 3.2, when h_0 intersects l_0, l_0 is always over h_0 by the convention in section 3.1. Moreover, since h_0 and l_0 do not have self-intersections, l_0 passes through D_h in parallel, disjoint segments. Therefore, l_0 and h_0 are "separable" by inverse Reidemeister type II moves alone.
- According to theorem 3.4 and figure 3.4(d), an inverse Reidemeister type II move of the *h-l* curves is realizable by Roseman moves at the cost of changing the *h-l* curves at other locations. In figure 3.4(d) corresponding to this situation, $a = l_0$ and $b = h_0$. Since h_0 and l_0 has no self intersections, h_1 and h_2 (and l_1 and l_2) cannot be the same curve as h_0 (and l_0). Therefore, such changes do not affect h_0 and l_0 at other locations. h_0 and l_0 are completely separable.

□

4.4 The self-intersecting case

In this section, another special case is discussed where h_0 has self-intersections and does not intersect with any other *h-l* curves and l_0 is a simple closed curve disjoint from h_0. The attempt, however, is more radical than a crossing change. It performs a surgery to the surface knot at the pair of "crossings" h_0 and l_0, removes a part of the surface and forms a new surface knot by gluing together the rest. Figure 4.13 shows an analogous surgery in knot theory.

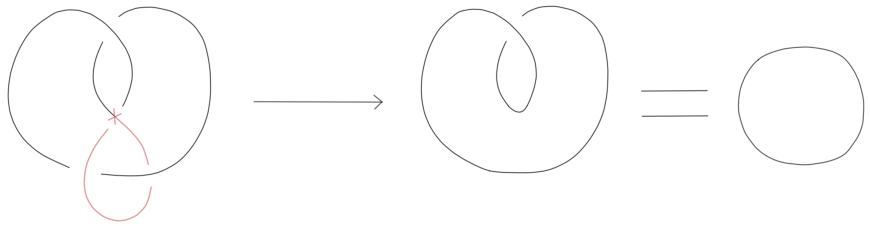

Figure 4.13: *A surgery in knot theory that removes part of the knot (the red part) and glues the rest together at a crossing*

For every pair of $p_i, q_i \in S^1$ such that $h_0(p_i) = h_0(q_i)$, there exists a pair of *h-l* curves a_i and $\tilde{a_i}$ such that l_0 intersects a_i at $l_0(p_i)$ and $\tilde{a_i}$ at $l_0(q_i)$. Figures 4.14 through 4.16 shows the surgery in steps.

Step 1

Let $D_l \subset S$ be the disc such that $\partial D_l = l_0$ and $h_0 \subset S - D_l$. Let $\tilde{D_l}$ be a larger disc containing D_l and disjoint from h_0, such that $\tau \circ K(\partial \tilde{D_l})$ is a self-intersecting, parallel copy of $\tau \circ K(h_0)$ in R^3. Let $l_1 = \partial \tilde{D_l}$ and parametrize l_1 by S^1 such that l_1 intersects the other *h-l* curves at the same positions as l_0 in the parametrization. (To avoid confusion, note that l_1 is not the name of an l curve.) Remove $\tilde{D_l}$ from S and $K(S)$. Denote $S_1 = S - \tilde{D_l}$. $\partial S_1 = l_1$. See figure 4.14.

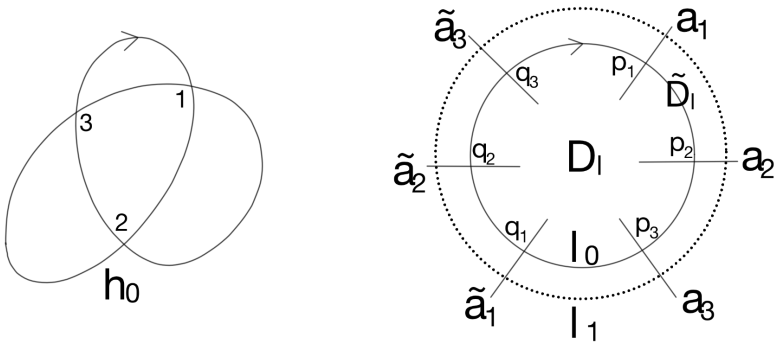

(a) *The h_0 and l_0 curves, and other notations*

Figure 4.14 (Continued on next page): *Illustration of Step 1, in the surgery to a self-intersecting h_0*

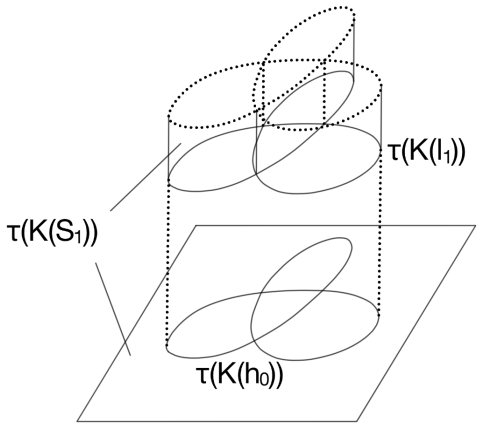

(b) *The resulting image of $\tau \circ K$ in R^3 after Step 1. Notice that $\tau \circ K(l_1)$, the boundary of $\tau \circ K(S_1)$, is a parallel copy of $\tau \circ K(h_0)$. There is no real intersection along $\tau \circ K(h_0)$ anymore after the removal of $\tau \circ K(\tilde{D}_l)$*

Figure 4.14 (Continued)

Step 2

For each $p_i, q_i \in S^1$ and the pair of h-l curves a_i and $\tilde{a_i}$ such that l_1 intersects a_i at $l_1(p_i)$ and $\tilde{a_i}$ at $l_1(q_i)$, attach a band $B_i \cong D^2$ to S_1 along two arcs $\alpha_i, \beta_i \subset l_1$ such that $l_1(p_i) \in \alpha_i$ and $l_1(q_i) \in \beta_i$ respectively, and α_i, β_i contains no other $l(p_j)$'s or $l(q_j)$'s. The orientation of B_i must match that of l_1. Denote $S_2 = S_1 \cup_i B_i$. See figure 4.15.

Define $\tau \circ K(B_i)$ as a Whitney umbrella bounded by $\tau \circ K(\alpha_i \cup \beta_i)$, following the orientations of α_i and β_i, and disjoint from $\tau \circ K(S_1)$. This defines $\tau \circ K(S_2)$.

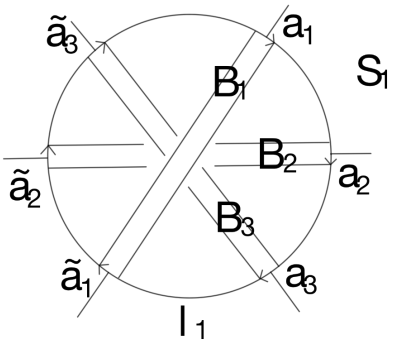

(a) S_2

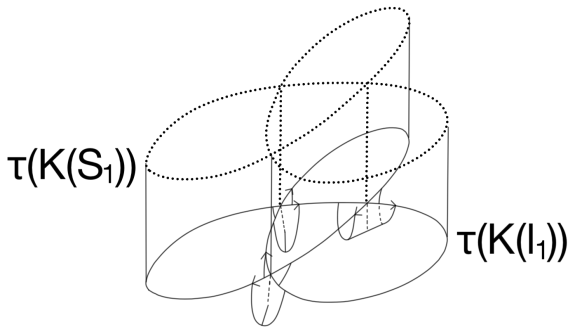

(b) *Part of $\tau \circ K(S_2)$ in R^3*

Figure 4.15: *Illustration of Step 2, in the surgery to a self-intersecting h_0*

Step 3

S^2 is homeomorphic to a 2-sphere with punctures. ∂S_2 is a collection of disjoint simple closed curves. $\tau \circ K(\partial S_2)$ is a collection of disjoint simple closed curves in R^3 that are parallel to $\tau \circ K(h_0)$, aside from the self-intersections of the latter. Make parallel copies of the disjoint discs in $\tau \circ K(S)$ bounded by the self-intersecting curve $\tau \circ K(h_0)$ and glue them to $\tau \circ K(\partial S_2)$. This completes the definition of the new surface knot in terms of its projection in R^3.

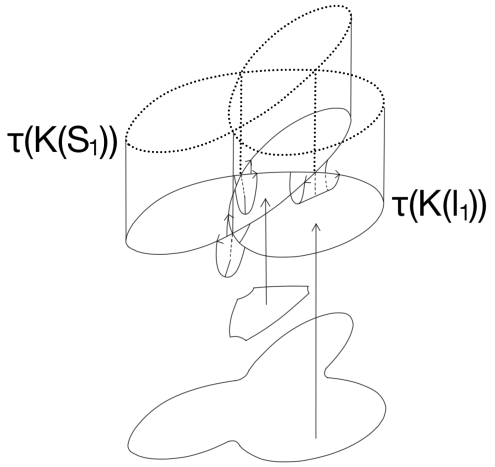

(a) *Step 3*

Figure 4.16: *Illustration of Step 3, in the surgery to a self-intersecting* h_0

The *h-l* curves of the new surface knot no longer contains the pair h_0 and l_0. Each pair of curves a_i and $\tilde{a}_i$ are connected in the new S by a branch point.

References

[Ada94] Colin C Adams. *The knot book*. American Mathematical Soc., 1994.

[Ale23] James W Alexander. A lemma on systems of knotted curves. *Proceedings of the National Academy of Sciences of the United States of America*, 9(3):93, 1923.

[Art25] Emil Artin. Zur isotopie zweidimensionaler flächen im r4. In *Abhandlungen aus dem Mathematischen Seminar der Universität Hamburg*, volume 4, pages 174–177. Springer, 1925.

[BZH13] Gerhard Burde, Heiner Zieschang, and Michael Heusener. *Knots*, volume 5. Walter de gruyter, 2013.

[Con70] John H Conway. An enumeration of knots and links, and some of their algebraic properties. In *Computational problems in abstract algebra*, pages 329–358. Elsevier, 1970.

[CS98] J Scott Carter and Masahico Saito. Surfaces in 3-space that do not lift to embeddings in 4-space. *Banach Center Publications*, 42:29–47, 1998.

[FM66] Ralph H Fox and John W Milnor. Singularities of 2-spheres in 4-space and cobordism of knots. *Osaka Journal of Mathematics*, 3(2):257–267, 1966.

[Fox62] Ralph H Fox. A quick trip through knot theory. *Topology of 3-manifolds and related topics*, 1962.

[Gil82] Cole Giller. Towards a classical knot theory for surfaces in r4. *Illinois J. Math*, 26(4):591–631, 1982.

[Kaw12] Akio Kawauchi. *A survey of knot theory*. Birkhäuser, 2012.

[Kaw20] Akio Kawauchi. Ribbonness of a stable-ribbon surface-link, i. a stably trivial surface-link. *Topology and its Applications*, page 107522, 2020.

[Kim20] Jieon Kim. An enumeration of immersed surface-links in 4-space. *Topology and its Applications*, 279:107241, 2020.

[KS82] Akio Kawauchi and Tetsuo Shibuya. Descriptions on surfaces in four-space, i. normal forms. *Math. Sem. Notes Kobe Univ.*, 10:75–125, 1982.

[KY15] A Al Kharusi and Tsukasa Yashiro. On crossing changes for surface-knots. *arXiv preprint arXiv:1506.02269*, 2015.

[Mil16] John Milnor. *Morse Theory.(AM-51), Volume 51*, volume 51. Princeton university press, 2016.

[Oga01] Eiji Ogasa. The projections of n-knots which are not the projection of any unknotted knot. *Journal of knot theory and its ramifications*, 10(01):121–132, 2001.

[Rei27] Kurt Reidemeister. Elementare begründung der knotentheorie. In *Abhandlungen aus dem Mathematischen Seminar der Universität Hamburg*, volume 5, pages 24–32. Springer, 1927.

[Ros98] Dennis Roseman. Reidemeister-type moves for surfaces in four-dimensional space. *Banach Center Publications*, 42:347–380, 1998.

[Ros04] Dennis Roseman. Elementary moves for higher dimensional knots. *Fund. Math*, 184:291–310, 2004.

[Sat00] Shin Satoh. Lifting a generic surface in 3-space to an embedded surface in 4-space. *Topology and its Applications*, 106(1):103–113, 2000.

[Sat02] Shin Satoh. Surface diagrams of twist-spun 2-knots. *Journal of Knot Theory and Its Ramifications*, 11(03):413–430, 2002.

[Tan04] Kokoro Tanaka. Crossing changes for pseudo-ribbon surface-knots. *Osaka Journal of Mathematics*, 41(4):877–890, 2004.

[Whi44] Hassler Whitney. The singularities of a smooth n-manifold in (2n-1)-space. *Annals of Mathematics*, pages 247–293, 1944.

[Yos94] Katsuyuki Yoshikawa. An enumeration of surfaces in four-space. *Osaka Journal of Mathematics*, 31(3):497–522, 1994.

[Zee65] E Christopher Zeeman. Twisting spun knots. *Transactions of the American Mathematical Society*, 115:471–495, 1965.